

Chapter 11

Co-operative Populations of Neurons: Mean Field Models of Mesoscopic Brain Activity

David T.J. Liley, Brett L. Foster, and Ingo Bojak

Abstract While the basic units of computation in the brain are the neuronal cells, their sheer number, complexity of structural organisation and widespread connectivity make it difficult, if not impossible, to perform realistic simulations of activity at millimetre range or beyond. Furthermore, it is becoming increasingly clear that a range of non-neuronal and stochastic factors influence neuronal excitability, and must be taken into account when developing models and theories of brain function. One answer to these persistent difficulties is to model cortical tissue not as a network of spike-based enumerable neurons, but to take inspiration from statistical physics and model directly the bulk properties of the populations constituting the cortical tissue. Such an approach proves compatible with many experimental recording techniques and has led to a successful class of so-called “mean field theories” that, when constrained by meaningful physiological and anatomical parameterisations, reveal a rich repertoire of biologically plausible and predictive dynamics. The aim of this chapter is to outline the historical genesis of this important modelling framework, and to detail its many successes in accounting for the experimentally observed neuronal population activity in cortex.

D.T.J. Liley (✉)
Brain Sciences Institute, Swinburne University of Technology, P.O. Box 218, Hawthorn,
VIC 3122, Australia
e-mail: dliley@swin.edu.au

B.L. Foster
Department of Neurology and Neurological Sciences, Stanford University, Stanford,
CA 94305, USA
e-mail: blfoster@stanford.edu

I. Bojak
Donders Institute for Brain, Cognition and Behaviour, Centre for Neuroscience, Radboud
University Nijmegen Medical Centre, Postbus 9101 // 126, 6500 HB Nijmegen, The Netherlands
e-mail: i.bojak@donders.run.nl

Not only is it not proven, but it is highly unlikely on general biological considerations, that a special sensory function is related to a cell type of a particular structure. The essential for the elaboration of any cortical function, even the most primitive sensory perception, is not the individual cell type but cell groupings.

Korbinian Brodmann (1909)

... the effective unit of operation in such a distributed system is not the single neuron and its axon, but groups of cells with similar functional properties and anatomical connections.

Vernon B. Mountcastle (1997)

11.1 Introduction

Ever since the formulation of the neuron doctrine by Santiago Ramón y Cajal, Rudolf von Kolliker and others (López-Muñoz et al. 2006), neuroscience has strived to understand how consciousness and cognition arises out of the myriad and complex interactions between neurons of the central nervous system. Beginning with the work of McCulloch and Pitts (1943), in which single neurons were conceived as simple fixed threshold binary state devices organized into networks of great structural complexity, and culminating in the massively detailed single neuron models of the Blue Brain Project headed by Henry Markram (2006), brain function has been assumed to emerge out of the activity of networks of neurons. This has been an enormously successful paradigm and has led to models of great computational complexity and sophistication. However, it is becoming increasingly clear that a range of non-neuronal and stochastic factors and elements influence neuronal excitability and that these must be taken into account when developing models and theories of brain function, if we are to meaningfully simulate emergent neuronal activity. For example, it is now known that the supporting non-neuronal elements of cortical tissue, the glial cells (Perea et al. 2009; Perea and Araque 2010), interact synaptically with cortical neurons to influence the patterns of neuronal firing. Further, while the firing of individual neurons is regulated by deterministic factors their synaptic interactions may well not be – the reliability of synapses can be as low as 1%, i.e., only 1 in 100 pre-synaptic action potentials actually elicits a postsynaptic response (Branco and Staras 2009).

The problem is how to deal with this significant added complexity in the presence of often limited and non-specific empirical data. One possible solution has been to *not* consider cortical tissue as an network of enumerable neurons interacting by the transmission of spikes, and instead consider cortex in terms of a bulk or ensemble dynamics, such as the mean firing rate (and/or its moments) of a spatially circumscribed population of neurons (Freeman 1975; Nunez 1995; Deco et al. 2008; Coombes 2010). Such a rate-based reconfiguration has a number of advantages: (1) modelling populations of neurons corresponds more closely with the generally accepted contention that behaviour emerges out of the macroscopic manifestations of neuronal activity, (2) modelling the behaviour of populations of

neurons implicitly deals with the unreliability of synaptic interconnections and incorporates the effects of non-neuronal elements, and (3) the spatial scale of modelled populations of neurons corresponds closely with the milli- to centimetre scales of spatial resolution of the non-invasive neuroimaging modalities typically utilised to interrogate brain function, like functional magnetic resonance imaging (fMRI), MEG (magnetoencephalogram) and EEG (electroencephalogram).

Describing cortical neuronal activity in terms of population averages gives rise to a class of models broadly known as mean field theories (Deco et al. 2008). Originally arising out of mathematical models of ferromagnetism in statistical physics, such models approximate the specific input a neuron receives from other neurons by the average activity in a neuronal surround defined by patterns of axonal and dendritic branching. In this way interactions between individual neurons are replaced by effective averages – the mean fields, i.e., cortical neurons can be viewed as “*sampling*” the activity of nearby populations of neurons based on the mean geometry of the axonal and dendritic arborisations. Thus the dynamics of populations of neurons are driven by mean fields, which are in turn determined by the activity of populations of neurons. The current mathematical approach for formulating equations of motion for the activity of neuronal populations or “masses” stems principally from the work of Wilson and Cowan (1972, 1973), Nunez (1974a), Freeman (1975) and Amari (1975, 1977). The resulting so-called mass action or neural field theories have formed a basis for the biomathematical exploration of macro- and mesoscopic neuronal dynamics. Mesoscopic neuronal activity is typically defined to be intermediate in scale between the activity of single neurons and the activity of large areas of cortex, i.e., at roughly millimetre scale.

The aim of this chapter is to outline in some detail the formulation of physiologically relevant mean field theories and how they can be utilised to account for a range of mesoscopic brain activity that includes the spatiotemporal dynamics of the resting EEG/electrocorticogram (ECoG), its perturbation during diseases such as epilepsy, and its modulation by a range of drugs that most importantly include anaesthetic and sedative agents. The chapter is organized into three main sections. The first describes the anatomical and physiological basis for modelling mesoscopic neuronal activity in mammalian cortex and the bulk and discrete approaches that have typically been employed to model it. It then focuses on the advantage of bulk approaches in the context of limited empirical knowledge and outlines the implicit microscopic constraints necessary in formulating the corresponding mean field theories. The second section outlines the existing mean field approaches by way of their historical development, firstly by describing the foundational models, and then their subsequent elaboration and development to include greater levels of physiological veracity. Finally, the third section details the patterns and types of mesoscopic brain activity that can provisionally be accounted for by the various mean field models.

11.2 Mesoscopic Neural Activity

Because the structure and function of the mammalian brain resists any simplistic representation or definition it has been difficult to conceive of generative theoretical frameworks to account for human behaviour on the basis of neural activity. The activity of human brains encompasses many aspects and spatial and temporal scales: from the millisecond flurry of the opening and closing of transmembrane ionic channels to socio-political machinations that can extend over many decades. Typically one wants to explain the behaviour observed at a higher, more meaningful level in terms of activity occurring at a lower, more mechanistically accessible level. In the case of neuroscience the long-term aim is to relate human intentional behaviour to the activity of neurons. However the gulf between the local actions of individual neurons (microscopic) and the intentional patterns of activity evinced by non-invasive neuroimaging modalities such as positron emission tomography (PET), single-photon emission computed tomography (SPECT) and fMRI (macroscopic) is too wide to bridge with current theories. An intermediate level of description is hence required. This mesoscopic level of the neuronal ensemble, mass or population is best justified on the basis of the anatomical structure of cortical tissue, which we proceed to outline, but can also be motivated using statistical mechanics (Deco et al. 2008).

11.2.1 Anatomical and Physiological Organization of the Cerebral Cortex at Different Scales

The thin outer rind of the mammalian brain, the neocortex, is generally thought to be the principle structure responsible for the generation and elaboration of purposeful activity. For a structure that is between 1 and 5 mm thick and has a surface area of only $\sim 0.19 \text{ m}^2$ (Van Essen 2005), it has a truly staggering degree of structural complexity with about $\sim 2 \cdot 10^{10}$ neurons (Pakkenberg and Gundersen 1997) divided into six horizontal layers with at least a dozen major neuronal subtypes (Markram et al. 2004), each interacting via on average 6,900 synaptic connections with other neurons (Tang et al. 2001), synapses that utilise an array of chemical messengers and can be individually modified. Add in the non-neuronal glia known to influence cortical neuronal activity (Ben Achour and Pascual 2010; Araque and Navarrete 2010), astrocytes and microglia, which are equivalent in number and density to the neurons (Miguel-Hidalgo 2005; Azevedo et al. 2009), then the task of simulating cortical neuronal activity appears daunting, if not intractable. Fortunately, mammalian cerebral cortex is sufficiently well organized over a number of relatively distinct spatial scales to enable the construction of tractable models and theories of brain activity beyond that of the enumerable neural network. Furthermore, despite great variations in the size of the cortex among

the various mammalian groups (Herculano-Houzel 2009), it nevertheless remains remarkably consistent in terms of its cellular elements, and its vertical and horizontal organization.

11.2.1.1 The Cellular Composition of Cortex

Cortex is comprised of neuronal and non-neuronal components with the neurons being broadly classified as belonging to two types: pyramidal and non-pyramidal cells. Pyramidal cells are the most numerous neuronal class making up somewhere between 60% and 85% (Braitenberg and Schüz 1998; Nieuwenhuys et al. 2008) of all cortical neurons. A typical pyramidal neuron is composed of a cell body from which a single axon descends and branches before exiting cortex, as well as a dendritic tree composed of two main branching structures (1) an apical dendritic tree composed of a trunk ascending in the direction of the pial surface and (2) a basal dendritic tree composed of multiple trunks giving rise to a cloud of local dendritic branches about the cell body. Both dendritic structures are typically extensively covered with small excrescences called spines where synapses form (Spruston 2008). Particularly in sensory cortices the apical dendrites of 50 or so pyramidal neurons distributed throughout the thickness of cortex can be clustered together into distinct and regularly spaced cylindrical groupings. These cylindrical groupings, referred to as dendrons by Eccles (1992), constitute a core component of the hypothesised “*minicolumn*”: a barrel shaped region representing the basic modular unit of neocortex (Rockland and Ichinohe 2004).

While pyramidal neurons generally show a fair degree of morphological variability the only atypical variant is the spiny stellate cell, an interneuron (see below) which lacks the characteristic ascending apical dendritic tree and descending axon. Pyramidal neurons constitute a functionally homogeneous group as they all exclusively release the excitatory monoamine glutamate from their axonal terminals. It is also worth noting that pyramidal neurons can be functionally subdivided based on their steady state firing pattern in response to step depolarising currents (Contreras 2004). As will be discussed later in Sects. 11.2.1.2 and 11.2.1.3, the branching pattern of pyramidal cell axons and the minicolumn form two possible characteristic scales for the spatial organization of cortex.

Despite their smaller numbers non-pyramidal cells are a morphologically much more differentiated class of cortical neuron that have a number of features in common (Nieuwenhuys et al. 2008): their dendrites are often spine free, their axons do not leave cortex (hence often called *local circuit* or *interneurons*), most release the inhibitory neurotransmitter γ -amino butyric acid (GABA) and a certain fraction (25–30%) also express one or more neuropeptides such as vasoactive intestinal polypeptide (VIP) or cholecystokinin, and various subpopulations show differential immuno-reactivity to one or more intracellular calcium binding proteins which can be used as subpopulation specific markers. It has been estimated that a dozen or so non-pyramidal cell sub-types can be identified morphologically (Markram et al.

2004), the most numerous of which are basket cells, whose axons form basket-like plexuses around pyramidal cells bodies, Martinotti cells, which project their axons to the superficial layers of cortex to interact with apical dendrites of pyramidal neurons, and bitufted cells, which have dendrites arising from upper and lower poles of the cell body.

Other notable non-pyramidal cells include the Chandelier, bipolar and double bouquet cells. Chandelier cells produce a profusely ramifying axonal tree with “candles”, short vertical axonal segments containing rows of synaptic boutons, that are the pre-terminal components of axo-axonic synapses at initial segments of pyramidal neurons. Bipolar neurons, which are similar in morphology to bitufted neurons, represent the single known example in which a non-pyramidal neuron can be excitatory by releasing only VIP. They can also be inhibitory by releasing only GABA, while also expressing VIP (Markram et al. 2004). Double bouquet cells have a similar dendritic morphology to bitufted cells but produce radially (vertically) oriented dense axonal plexuses consisting of bundles of thin parallel axonal branches. Because the axonal system of a single double bouquet cell is closely associated with the apical dendrites of pyramidal neurons in a minicolumn and has a relatively well defined lateral extent of arborisation, their spacing (30–50 μm) provides a characteristic tangential (horizontal) scale for cortical organization. Like pyramidal neurons the non-pyramidal neurons can also be electrophysiologically classified.

The non-neuronal components of cortical tissue can be divided into the neuroglia and the cells of the perforating blood vessels. The neuroglia are comprised of astrocytes, microglia, oligodendrocytes and ependymal cells. Classically it used to be thought that the activity of these neuroglia did not contribute in any meaningful way to brain function: astrocytes, star shaped cells with multiple processes, provided biochemical, metabolic and structural support to the neurons and their interactions; microglia are the brain’s macrophages; oligodendrocytes produced the myelin sheaths around axons to increase conduction velocities; and epithelial ependymal cells lining the ventricles produced the cerebral spinal fluid. However, beginning in the early 1990s research has revealed that astrocytes, like neurons, are excitable (with respect to intracellular Ca^{2+} levels) and respond to, and are influenced by, neuronal activity at the level of the synapse. To conceptualise this evidence the term “tripartite synapse” has been proposed (Perea et al. 2009), defined as consisting of one or more glial processes chemically interacting with the pre- and post-synaptic components of a synapse. Such ‘synapses’ seem to occur at the synapses of all neurons in cortex and have been shown to regulate interneuronal synaptic transmission and plasticity. Given these interactions and the fact that astrocyte–astrocyte interactions can be demonstrated (Dienel and Cruz 2003), it follows that functionally cortical tissue is more than just a network of neurons.

11.2.1.2 Vertical/Radial Organization of Neocortex

Beginning with Theodor Meynert and Vladamir Betz and culminating in the 1909 work of Korbinian Brodmann (Brodmann and Garey 2006), cerebral cortex was

found to be divided into vertically stacked cellular laminae, the number, size and organization of which show substantial horizontal (regional) variation.¹ From an ontogenetic (developmental) perspective two broad structural forms of cerebral cortex can be identified based on the genesis of their laminar organization – homogenetic cortex and heterogenetic cortex. Homogenetic cortex, which is more commonly referred to as neocortex or isocortex, makes up the bulk of cerebral cortex and either consists of six reasonably well defined cellular laminae (homotypical cortex) or began as a six-layered cortex but during development addition or elimination of layers occurred (heterotypical cortex). In contrast, heterogenetic cortex is divided into primitive (or paleo-) cortex, in which there is no clear laminar cellular organization, and rudimentary (or archi-) cortex, in which there are only the crude beginnings of lamination. The olfactory bulb and amygdala are examples of paleocortex, whereas the hippocampus is an example of archicortex, in which there are only three identifiable cellular layerings.

The six neocortical layers labelled I–VI, see Fig. 11.1, are characterised by variations in cellular densities, types and morphologies as well as the patterns of termination and generation of cortical and subcortical afferents and efferents. Non-pyramidal cells occur in all layers and pyramidal cells in layers II–VI. Layer IV of sensory cortices is notable for the large numbers of tightly packed spiny stellate neurons, which are only found there, and the termination of sensory thalamocortical afferents on these neurons and the dendrites of other neurons passing through this layer (Thomson and Bannister 2003). In contrast it has been observed that associational and callosal cortico-cortical efferents arising from layer II and III pyramidal neurons preferentially terminate in layers IV, whereas layer V/VI pyramidal neuron long-range axons preferentially terminate in layers I and VI (Rockland and Pandya 1979).

While such cortical lamination suggests discrete horizontally arranged neuronal populations, such a distinction becomes less convincing when other radially organized cortical elements are included. Among the most (histologically) prominent of these are clusters or bundles of apical dendrites of layer V pyramidal neurons (Fleischhauer et al. 1972), bundles of descending myelinated axons of pyramidal cells generally referred to as the “radiations of Meynert” and column-like arrays of pyramidal cell bodies thought to be direct developmental descendants of organized clusters of cells in the embryonic precursor of the cerebrum. In addition, double bouquet interneurons (see Sect. 11.2.1.1), which are abundant in primate neocortex, give rise to tightly packed bundles of vertically oriented axonal collaterals called “horses tails” that span multiple laminae. Multiple radially organized cellular elements therefore bind pyramidal and non-pyramidal components across the various cortical laminae. Horizontal (or areal) periodicities in the radial organization of these neocortical cellular elements may provide a structural basis for defining the modular organization of neocortex.

¹Here and in the following we mean by “vertically/radially” through the several millimetres thickness of cortex and by “horizontally/tangentially” parallel to its pial surface.

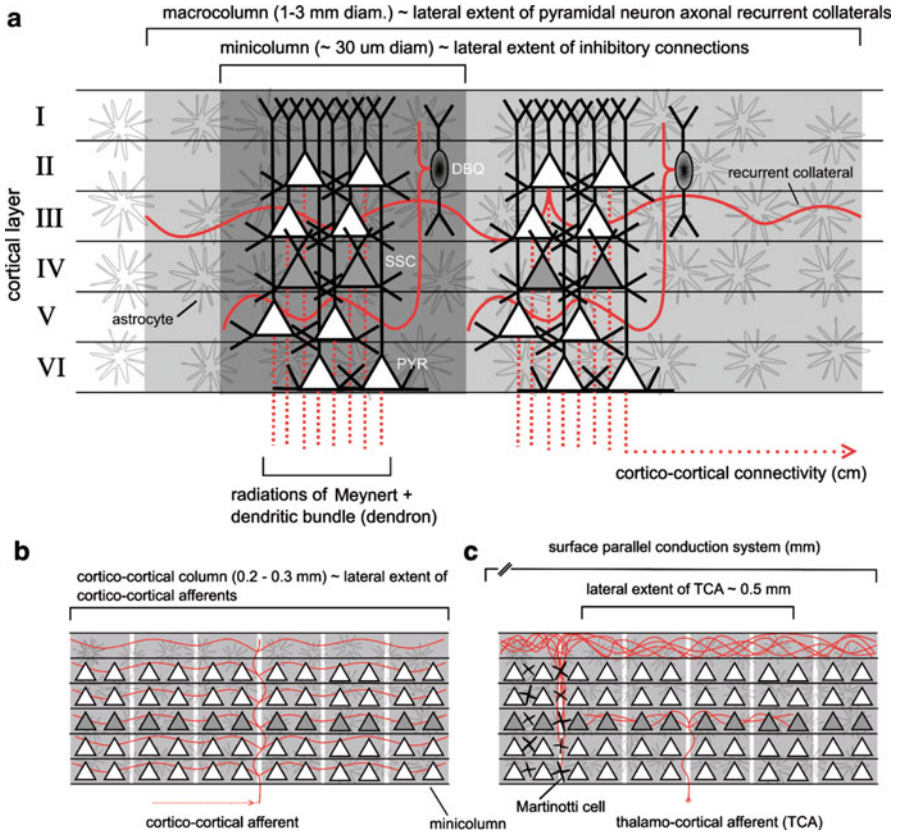


Fig. 11.1 Highly simplified sketch of the hypothetical modular organization of neocortical tissue. (a) The minicolumn was originally defined as a narrow chains of 100–200 neurons extending across layers II–IV and organized into repeating patterns (Mountcastle 1979). A variety of radially oriented units have a similar scale to the putative minicolumn. These include pyramidal (PYR) cell dendritic (dendron) and axonal (radiations of Meynert) bundles, as well as lateral arborisations of double bouquet neurons (DBQ). A macrocolumn binds together laterally about thousand minicolumns by recurrent axonal collaterals of an intracortical pyramidal axon. (b) The cortico-cortical column is defined by the lateral extent of intracortical terminations of afferent cortico-cortical fibres (associational and callosal). (c) Other hypothetical scales of modular organization include the lateral extent of thalamocortical afferents, shown here to principally synapse with spiny stellate cells (SSC), and the layer I plexiform arborisations of the axons of inhibitory Martinotti neurons

11.2.1.3 Horizontal/Tangential Organization of Neocortex

The idea that cortex is horizontally parcellated into anatomically well defined radially oriented columnar units has become virtual dogma. Commencing with the work of Lorente de N6, who first proposed that a small radially oriented cylinder

of cells extending through the full extent of cortex with a single thalamocortical axon as its axis defined an “*elementary unit*” of neocortical organization, the intervening years have seen a panoply of attempts to define a “*basic modular unit*” of cortical organization. Amongst the most well known are the micro-, mini-, macro- and cortico-cortical columns. Micro- and minicolumns typically refer to radially organized chords of ≈ 10 – 200 cells that span layers II–VI, arranged as horizontal mosaics with periodicities of the order of 15 – $80\ \mu\text{m}$ (Jones 2000; Buxhoeveden and Casanova 2002; Rockland and Ichinohe 2004; Nieuwenhuys et al. 2008). In addition, there are a range of other elements repeating at this scale that could be said to define micro-/macrocolumnar organization. These include the periodically repeating bundles of radially oriented dendrites (pyramidal cell) and axons (double bouquet) mentioned above.

Columns were first hypothesised by Mountcastle (1957) on the basis of electrophysiological evidence in which radially co-localized neurons in cat somatosensory cortex shared receptive field properties in response to tactile stimulation. The lateral extent of this shared receptive field was estimated to be of the order of $0.5\ \text{mm}$. These columns, later designated macrocolumns (Mountcastle 1979), were subsequently considered by Mountcastle to be anatomically comprised of aggregations of several hundred minicolumns bound together by short range horizontal excitatory and inhibitory connections (Mountcastle 1997). In contrast to macrocolumns whose lateral extent is defined by the scale of short range horizontal connectivity, cortico-cortical columns (also referred to as neocortical columns) are typically defined in terms of the cylindrical aborisation volumes of either a single afferent cortico-cortical fibre or closely packed bundles of such fibres (Jones et al. 1975; Goldman and Nauta 1977; Szentágothai 1983). Estimates of the radial extent of such columns varies from 200 to $800\ \mu\text{m}$.

While some areas of cortex have a greater claim to displaying some form of columnar organization than others, visual and somatosensory in particular, cortical columns of any form or variety have not been substantiated by unequivocal anatomical evidence and therefore remain hypothetical. Neocortical columns (Markram 2008), intensely studied in barrel cortex (Petersen 2007; Lübke and Feldmeyer 2007), are perhaps closest to being established. What however is abundantly clear is that neocortex consists of populations of vertically well connected cellular elements interacting horizontally over a range of spatial scales. In general it is the lateral axonal ramifications of neocortical pyramidal neurons that define the spatial scales of horizontal connectivity within neocortex. The axons of all typical (i.e., not spiny stellate) pyramidal cells produce a number of horizontal branches (collaterals) in cortex before entering subcortical white matter where they form the long-range cortico-cortical fibres systems (see Fig. 11.1). Intracortical horizontal branches can either ramify in close proximity to the parent cell body or travel laterally for many millimetres depending on species, cortical area and layer (Nieuwenhuys et al. 2008). In general, it appears that the longer the branch the more likely it is to be myelinated.

Pyramidal axonal collaterals provide local input to GABAergic interneurons, which in turn form reciprocal synapses with pyramidal neurons (White 1989). In contrast, cortico-cortical axons can travel for many centimetres in subcortical white

matter before re-emerging in cortex to form synaptic connections with all neuronal cell types, and in particular with the apical dendrites of typical pyramidal neurons. The cortico-cortical system of connectivity can be divided into commissural and associational fibre systems, depending on whether they respectively pass through the corpus callosum or remain ipsilateral. Somewhat arbitrarily, associational fibres can be divided into short- and long-range. The short-range system is believed to be fairly isotropic and homogenous in its distribution, while the long-range one is readily identified from gross dissection and non-invasive tractographic methods based on diffusion MRI (Johansen-Berg and Rushworth 2009). In humans the majority of commissural axons are myelinated (Aboitiz et al. 1992a,b) and based on measurements of fibre diameter are expected to have broadly distributed range of conduction velocities (Bojak and Liley 2010). Anatomical evidence suggests that the density of excitatory synapses arising from cortico-cortical afferents is similar to those made by recurrent axonal collaterals (Liley and Wright 1994; Braitenberg and Schüz 1998).

The lateral axonal ramifications of certain interneurons provide additional characteristic scales for the horizontal organization of cerebral cortex. We have encountered one such interneuron type previously – that of the layer II/III double bouquet cell whose descending bundles of axons have been shown to disperse horizontally in deeper layers. Peters and Sethares (1997) have estimated that the spacing of these so-called “horse tails”, and by inference the extent of their terminal axonal arborisations, is 23 μm in rhesus monkey primary visual cortex. Another interneuron cell type that has been described as giving rise to extensive lateral axonal arborisations is the Martinotti cell. Martinotti cells, which occur in layers II–VI give rise to one or more ascending axons that project to laminae I, where they give rise to long horizontal branches that can run for several millimetres making synapses with the apical dendrites of pyramidal neurons. Szentágothai (1978) defined the “*surface parallel intracortical system*” to be comprised of these axons.

In addition, there have been attempts to topographically parcellate cerebral cortex according to shared anatomical, histological or histochemical features. The most consequential of these are those concerned with horizontal (areal) variations in the cellular architecture of the various neocortical laminae (cytoarchitectonics), in the organization of radially oriented bundles of myelinated fibres called *radii* or *radiations of Meynert* (myeloarchitectonics) and in the temporal order in which subgriseal white matter becomes myelinated during development. Of these architectonic parcellations the 1909 Brodmann map is still widely used (Zilles and Amunts 2010). By observing differences in the relative thickness and cell density of various layers and the size, shape and arrangement of neuronal cell bodies, Brodmann delineated 44 (paired) areas in the human neocortex (Nieuwenhuys et al. 2008; Brodmann and Garey 2006). However, because he and others only used a single stain (Nissl) and a limited number of brains, determined areal boundaries subjectively and ignored sulcal cortex, Nieuwenhuys et al. (2008) conclude that existing architectonic parcellations may substantially underestimate the number of juxtaposed structural areas. For example, modern approaches provide probabilistic maps of eight subdivisions of Brodmann areas 5 and 7 in the human superior parietal

Table 11.1 Major structural units of organization in mammalian neocortex and their approximate characteristics, see text

	Unit	Neurons per unit	No. of units ^b	Scale
Micro	Neuron (soma)	1	$2 \cdot 10^{10}$	15 μm
	Microcolumn ^a	20	10^9	15 μm
	Minicolumn	100	$2 \cdot 10^8$	35 μm
Meso	Dendritic tree	–	–	0.15 mm
	Cortico-cortical column	10^4	$2 \cdot 10^6$	0.35 mm
	Intracortical axonal tree	–	–	0.5 mm
	Macrocolumn	$2 \cdot 10^5$	10^5	1.5 mm
	Martinotti axonal tree	–	–	2 mm
Macro	Architectonic area	$2 \cdot 10^8$	100	5 cm ^b
	Cortico-cortical axon	–	–	10 cm ^b
	Brain region	$2 \cdot 10^9$	10	15 cm ^b
	Neocortex	$2 \cdot 10^{10}$	1	50 cm ^b

The table has been adapted from [Nunez \(1995\)](#), [Jones \(2000\)](#), [Buxhoeveden and Casanova \(2002\)](#) and [Nieuwenhuys et al. \(2008\)](#).

For neuronal groupings the diameter of a disk with equivalent cortical surface area is given as scale.

^aThe term “microcolumn” is sometimes used to refer to our “minicolumn”.

^bFigures are given for the human neocortex.

cortex ([Scheperjans et al. 2008](#)). The future of brain mapping efforts however likely belongs to comprehensive multimodal approaches, which for example integrate MRI data ([Toga et al. 2006](#)).

Table 11.1 summarises the various horizontal scales that have been identified or proposed on the basis of anatomical evidence. Based on this, and for the purposes of what follows, we choose to define the microscopic scale as commensurate with the level of the single neuron, micro- and minicolumn, whereas we establish the macroscopic scale as corresponding to the scale of the variously identified cyto/myelo-architectonic areas or larger. The mesoscopic level will thus represent an intermediate spatial scale including cortico-cortical and macrocolumns.

11.2.2 *Enumerable Network vs. Bulk Modelling Approaches*

The principle cellular substrate underlying brain function is without doubt the cortical neuron. On this basis, the most logical way forward to understanding the emergence of brain function is to simulate the activity of networks of neurons by modelling the properties and features of the individual neurons and the micro-circuitry of their connectivity. Yet such a research program faces a number of theoretical and practical problems: There are good reasons to believe that non-neuronal components of the brain, like the cortical astrocytes, play an important role in regulating interneuronal interactions, and thus neuronal activity.

Furthermore, cooperative neuronal activity dominates non-invasive measurements (e.g., EEG/MEG, fMRI BOLD) but often transcends the activity of the individual neuron. Practically, we have the problem of knowing how much detail to include – if the behaviour of individual neurons is believed crucial to understanding say the EEG, then the behaviour of individual ionic channels may be crucial to understanding the behaviour of individual neurons, and so forth. We soon find that trying to understand the behaviour of cortical tissue in terms of enumerating the functionally important components and their interactions leads to a combinatorial explosion in complexity. This is quite the opposite to what we want to achieve using modelling. Fortunately there is a way out of this epistemological bog.

Just as Waage and Guldberg in 1864 (Waage et al. 1986) sought to understand the kinetics of chemical reactions in bulk terms by defining the *principle of mass action* so a range of researchers, most notably Freeman (1975), have attempted to understand the dynamics of cortical neural activity in terms of the bulk interactions of functionally circumscribed masses or populations of neurons. The motivation for such masses in cortex depends upon two well established physiological principles: (1) firstly the vast majority of neurons in cortex chemically communicate using only a single neurotransmitter, and (2) the radial and horizontal organization of cortex (Sects. 11.2.1.2 and 11.2.1.3) defines domains of co-operative neural activity by virtue of synaptic interactions. Thus we can view cortex, at mesoscopic spatial scales, as networks of interacting populations or masses of excitatory (typical and atypical pyramidal) and inhibitory (non-pyramidal) neurons. In this way the cortical microcircuit is replaced by, and subsumed into, a *cortical mesocircuit*, see Fig. 11.2.

11.2.3 *Population Densities, Mean Fields, and Continuum Approaches*

One way forward to quantifying the dynamics of cortical mesocircuits is the ensemble density approach in which the time evolution of the probabilistic behaviour of large, potentially infinite, populations of neurons is quantified under the action of particular kinds of physiologically defined “*forces*” (Deco et al. 2008). Such an approach can include known stochastic fluctuations, such as variations in quantal transmitter release, as well as dynamically evolving the probability distributions associated with neuronal ensemble dynamics with all their moments and couplings. While providing a potentially rigorous approach to quantifying the dynamics of neuronal populations, in the context of empirical measurement problems arise: Firstly, probabilistic evolution, particularly in the presence of non-linearity, depends sensitively on initial states which in biological systems are in general unknowable. Secondly, actual measurements of the behaviour of populations of neurons will in general reflect only certain moments of the corresponding probability distributions, most prominently first moments (i.e., means). For example, a single EEG electrode records synaptically induced currents averaged over many thousands of neurons.

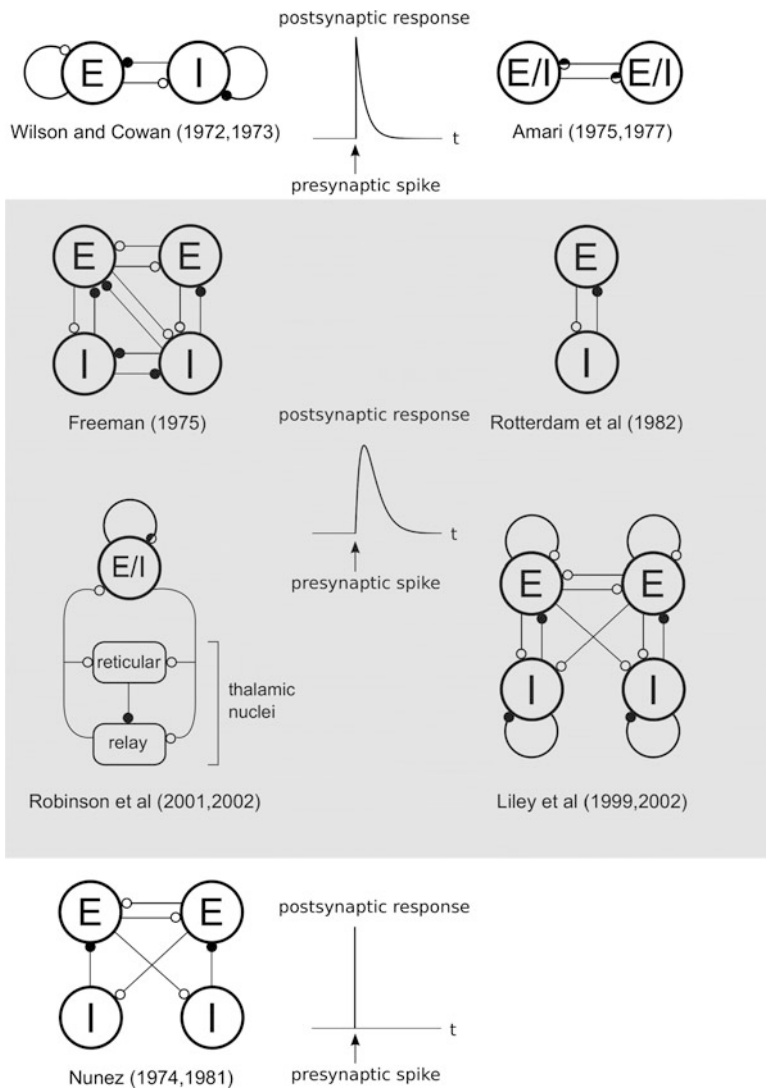


Fig. 11.2 Schematic representation of the circuit topologies of typical mean field models, segregated by their model for the postsynaptic response. All approaches consider two functionally differentiated neuronal populations: excitatory (E) and inhibitory (I) ones. *Open circles* represent excitatory connections, *filled circles* inhibitory ones, and *half-filled circles* both

For this and other reasons (Deco et al. 2008), approaches in which the dynamics of some appropriately defined first moment are tracked are often preferable. Such quantities typically include the “mean soma membrane potential” (Liley et al. 2002, 2003) and the “mean firing rate” (Wilson and Cowan 1972, 1973) of appropriately defined neuronal ensembles. These can be defined as either time- or

space-averaged, depending on the what spatiotemporal scales are intended to be modelled. For example, the passive membrane time constant of single neurons can furnish a characteristic time scale for the construction of a time-averaged neuronal ensemble; whereas the scale of intracortical connectivity or columniation can define a characteristic scale for space-averaged neuronal ensembles. Usually the averaging is performed over either time or space, but not both, leaving the respective other dimension at (theoretically) infinite resolution.

In the case that averaged neuronal ensembles are considered as localized, separable populations, the resulting formulations are often referred to as “*neural mass (action) models*”. These neural masses can be connected in a one-to-one fashion in order to represent their causal influence on each other through synaptic connectivity. However, neurons in cortex communicate with a very dense collection of short and long range fibres; hence it is often advantageous to envisage the activity of neuronal ensembles as conditioning entire regions of cortical space to a degree varying with connectivity. The mean activity of a particular neuronal ensemble then defines a distributed causal influence, a field, that is propagated and dispersed in a manner representing the dense synaptic connectivity. All other neuronal ensembles that are connected to it region are then subject to “forcings” from this field. The resulting models, which are continuous in space and time, are therefore referred to as “*neural/mean field models*”.

11.2.4 Microscopic Constraints on Mean Field Models

The strength of the mean field approach is also its weakness. Mean fields make the complexity of the cortex tractable, but do so at the expense of subsuming the effects of fluctuations and correlations in single neuronal activity that are known to affect emergent mesoscopic and macroscopic neuronal population dynamics (Wolfe et al. 2010). For instance, in a synergetic perspective (Haken 1983), the effects of upwards (microscopic \rightarrow mesoscopic \rightarrow macroscopic) and downwards (macroscopic \rightarrow mesoscopic \rightarrow microscopic) causation, and the feedback between the two (circular causality), are believed to be crucial in accurately understanding the dynamics of multiscale neural architectures. This cannot be included into mean field models without making a range of additional assumptions that have, at present, only weak physiological support. Nevertheless, mean field models do provide a convenient starting point through the study of first and possibly second order moments (Faugeras et al. 2009; Buice et al. 2010).

11.3 History of Mean Field Innovations

The earliest models of neural mass action applied to the cortex that attempted to describe the spatial and temporal behaviour of these aggregate masses dealt mainly,

if not exclusively, with excitatory interactions. Later models incorporated inhibitory interactions, paying more attention to the anatomical topology of connections between the neural masses, and took into account the conversion of efferent axonal activity into afferent dendritic activity (and the converse process), dendritic integration, axonal dispersion and synaptic delays. In what follows we will look at these developments in their historic context.

11.3.1 Foundations: Beurle, Griffith, Wilson and Cowan, Amari, Freeman

Perhaps the first approach to developing a mean field continuum theory of neural activity is that of [Beurle \(1956\)](#). In this theory, continuously distributed populations of excitatory neurons having a fixed firing threshold were considered in which the strength of interaction between individual neurons falls off exponentially with distance. By focusing on the fraction of excitatory neurons becoming active per unit time Beurle was able to show that this spatially continuous neural mass could produce propagating macroscopic waves of activity. While introducing a formalism that would later prove to be of great utility, the omission of inhibitory interactions meant its behaviour would be of no subsequent physiological significance. The later theory of [Griffith \(1963, 1965\)](#) suffered from the same problem, though he briefly discusses incorporating the influence of inhibition. However, his work is most notable for providing the first comprehensive derivation of a model for the spatiotemporal spreading of activation by using an equivalent partial differential equation (PDE). It was only through the later introduction by [Jirsa and Haken \(1996\)](#) of essentially the same idea that this approach became commonplace. We will discuss this in more detail below. The lack of an inhibitory component was subsequently rectified by the efforts of [Wilson and Cowan \(1972, 1973\)](#), [Amari \(1975, 1977\)](#) and [Freeman \(1975\)](#), who explicitly modelled inhibitory interactions.

[Wilson and Cowan \(1972, 1973\)](#) modelled cortical (and thalamic) neural tissue as comprised of two interacting, but functionally distinct, excitatory and inhibitory neuronal populations. The state of their bulk neuronal population model neural tissue was defined in terms of the time-averaged fraction of excitatory, $E(t)$, and inhibitory, $I(t)$, neurons firing per unit time, following the work of [Beurle \(1956\)](#). For point neural masses they were able to derive the following equations of motion

$$\tau_E \frac{dE}{dt} = -E + (1 - r_E E) S_E [c_{EE} E(t) - c_{IE} I(t) + P(t)] \quad (11.1)$$

$$\tau_I \frac{dI}{dt} = -I + (1 - r_I I) S_I [c_{EI} E(t) - c_{II} I(t) + Q(t)] \quad (11.2)$$

where $\tau_{E,I}$ are nominally the membrane time constants of the respective neural populations and determine their characteristic response times to incoming activity. The corresponding absolute refractory periods are denoted by $r_{E,I}$. The connectivity

coefficients $c_{EE,IE,EI,II} \geq 0$ quantify the interactions, whereas the functions $S_{E,I}$ describe the relationship between neuronal population input and output in the absence of refractory effects. Because firing rates are bounded below by a zero and above by some physiological maximum, the $S_{E,I}$ are typically chosen as sigmoidal functions of their arguments e.g. $S_E \equiv 1/(1 + \exp[-a(E - \theta_E)])$. $P(t)$ and $Q(t)$ define the external input to the excitatory and inhibitory sub-populations.

While no analytical solutions exist for these equations they can, like most two-dimensional nonlinear systems, be analysed qualitatively in the phase plane. A considerable body of work has been devoted to such analyses of Eqs. 11.1 and 11.2, determining the number, type and properties of the equilibria of the system, bifurcations, and the behaviour of multiply coupled Wilson-Cowan type systems. For an in depth review of these results and related modelling approaches see [Ermentrout \(1998\)](#). The work of [Wilson and Cowan \(1972, 1973\)](#) introduced a number of conceptual innovations that virtually all subsequent mean field formulations have retained: the sigmoidal firing rate function and the cortical mesocircuit defined by all possible feedforward and feedback connections between spatially circumscribed populations of excitatory and inhibitory neurons. In the Wilson and Cowan model, equations of motion for time-averaged neuronal firing rates were derived. This and related models are therefore referred to as *activity based* models. However there also exists an alternative way of formulating mean field, or continuum, models, referred to as *voltage based* models. These are arguably more pertinent to modelling, and thereby understanding, the genesis of EEG dynamics. In this modelling approach the resulting equations of motion instead describe the spatiotemporal evolution of the average membrane potential of neurons.

One of the biomathematically most influential *voltage based* continuum models of cortical dynamics is that of [Amari \(1975, 1977\)](#). In its most general form, this model considers m distinct spatially distributed neuronal populations, in which the average membrane potential impulse response to incoming (axonal) input from other neuronal populations is $\exp[-t/\tau]$. The resulting field equations can then be written as

$$\tau_i \frac{\partial u_i}{\partial t} = s_i(\mathbf{x}, t) - u_i(\mathbf{x}, t) + \sum_{j=1}^m \int dt' \int d\mathbf{x}' w_{ij}(\mathbf{x}, \mathbf{x}'; t - t') f_j[u_j(\mathbf{x}', t')] \quad (11.3)$$

where $u_i(\mathbf{x}, t)$ is the average membrane potential of neurons of type i at time t and position \mathbf{x} , s_i represents extracortical input and f_i is a nonlinear function that describes the average firing rate (pulse emission rate) as a function of u_i . The functions $w_{ij}(\mathbf{x}, \mathbf{x}'; t - t')$ define the strength of connectivity between neuronal populations, i.e., they determine the input to neurons of type i at \mathbf{x} from the pulse emission rate of neurons of type j at \mathbf{x}' , incorporating the effects of conduction and synaptic delays $t - t'$. As will be discussed below, the delay dependence is often factored out or simply ignored. The resulting function $w_{ij}(\mathbf{x}, \mathbf{x}')$ is then referred to as the *synaptic footprint*. A further common simplification is to consider the synaptic footprint as function of only the distance $r = |\mathbf{x} - \mathbf{x}'|$. The function $w(r)$

is then often defined to be excitatory $w(r) > 0$ (inhibitory $w(r) < 0$) for some defined neighbourhood $r < r_0$ and inhibitory $w(r) < 0$ (excitatory $w(r) > 0$) for more distant neurons $r > r_0$; this pattern of connectivity is typically referred to as (*inverted*) *Mexican hat connectivity*. For a detailed review of Amari-type models and their dynamics the reader is encouraged to consult [Coombes \(2005\)](#).

In contrast to the previous mathematical and constructive approaches, [Freeman \(1975\)](#) developed a schematic but empirically constrained mass action framework in order to explain the electrocortical dynamics of the mammalian olfactory bulb and pre-pyriform cortex. He developed a hierarchy of neural interaction – the well-known *K*-set hierarchy – in which functionally differentiated populations of neurons interact over progressively larger physical scales. The purpose of this hierarchy was to facilitate a more systems-oriented description. The simplest form of neural set that Freeman considered was the non-interactive or *KO* set. Members of this set have a common source of input and a common sign of output (excitatory or inhibitory), but do *not* interact synaptically or by any other means with co-members. At this level the characteristic form of the neuronal population response to incoming activity is specified. Unlike the first-order response of Wilson and Cowan, Eqs. 11.1 and 11.2, or Amari, Eq. 11.3, Freeman argued on the basis of detailed experiment that these population responses (or in his terminology “*pulse-to-wave*” conversion) could be described by third-order linear, time invariant, differential equations.

The *K*-set hierarchy was next extended to a non-zero level of functional interaction between members of the set. This defines the *KI* sets, broadly divided into mutually excitatory KI_e and inhibitory KI_i types. When there exists dense functional interaction between two *KI* sets, a *KII* set is formed. All possible interactions are in principle allowed to occur between the *KI* members of a *KII* set, which can be viewed as some local part of neocortex. The *K*-set hierarchy extends similarly to *KIII* and *KIV* sets, which nominally correspond to cortical areas and regions. The *KII* set of Freeman is equivalent physiologically and anatomically to the topology of cortex considered by Wilson and Cowan. Mathematically, the *KII* set is defined by four nonlinearly coupled sets of third order differential equations. The nonlinear couplings define how the induced population response to incoming synaptic activity is transduced into a neural population firing rate output. [Freeman \(1979\)](#) referred to the corresponding nonlinear function as the “*wave-to-pulse*” conversion function and has argued that such a function is an asymmetric sigmoid of the form $f(v) \propto \exp[-a \exp(-bv)]$.

11.3.2 *Synaptic Dynamics: Lopes da Silva, Jansen and Rit, Wendling*

While early models were successful in elaborating a cortical mesocircuit suitable for mean-field and mass action modelling, with the exception of [Freeman \(1975\)](#) they unrealistically assumed that the effects of synaptic activity are felt instantaneously at the neuronal soma. However, experiment suggests that the response of the neuronal

membrane potential (and by inference the average membrane potential of a neuronal population) to incoming pre-synaptic spikes is at the very least second order: membrane potential rises to a peak and then decays away with characteristic time courses (Kandel et al. 2000). These “impulse” responses are referred respectively to as excitatory (EPSP) or inhibitory postsynaptic potentials (IPSP), depending on whether the spike arose from an excitatory or inhibitory neuron. Freeman (1975) calls this transduction of pre-synaptic activity into post-synaptic (soma) membrane variation “*pulse-to-wave*”. Such PSP delays are thought, on both empirical and theoretical grounds, to be important in defining the characteristic time scales of a range of electrocortical oscillatory phenomena that include alpha (8–13 Hz) and gamma (>30 Hz), and their modulation by, e.g., anaesthetic agents.

Probably the first to explicitly include PSPs in a mean field model were Lopes da Silva et al. (1974), cf. van Rotterdam et al. (1982), who constructed a bulk model of the EEG in which lumped or spatially distributed populations of excitatory and inhibitory neurons synaptically interacted via EPSPs and IPSPs having the form $PSP(t) = V_{PSP} t \exp[-t/\tau_{PSP}]$, and where the mean neuronal population firing rate was a nonlinear (sigmoidal) function of the average membrane potential. The inclusion of such lumped postsynaptic dynamics was found sufficient to produce oscillatory activity in the alpha (8–13 Hz) electroencephalographic band. Jansen and Rit (1995), in a comprehensive extension of this model, investigated systematic variations of the model PSP parameters in order to account for observed changes in the visual evoked potential. Others have sought to better define the shape of the PSP in terms of a bi-exponential $PSP(t) \propto \exp[-t/\tau_1] - \exp[-t/\tau_2]$ with $\tau_1 > \tau_2$, see for example Robinson et al. (2001) and Bojak and Liley (2005), or included IPSPs with different time scales in order to incorporate the effects of fast (GABA_A) and slow (GABA_B) inhibitory neurotransmitter kinetics (Wendling et al. 2005).

11.3.3 Activity Propagation: Nunez, Wright and Liley, Jirsa and Haken, Bojak and Liley

Consider a signal $S_j(\mathbf{x}', t')$, for example a brief “pulse” of excitatory ($j = e$) activity $S_e(\mathbf{x}', t') = \delta^{(2)}(\mathbf{x}' - \mathbf{x}_0)\delta(t' - t_0)$ which is generated at $t' = t_0$ and $\mathbf{x}' = \mathbf{x}_0$. How does this signal, and others generated in the brain, relate to the input received by a neural population k at position \mathbf{x} and time t ? A general expression is

$$\phi_{jk}(\mathbf{x}, t) = \int dt' \int d\mathbf{x}' \mathcal{G}_{jk}(\mathbf{x}, \mathbf{x}', t, t') S_j(\mathbf{x}', t'), \quad (11.4)$$

i.e., an integration of signals from all times t' and places \mathbf{x}' with a function \mathcal{G}_{jk} weighting how much these signals contribute to the input. For a discretized model the integrals would be replaced by sums. The impact of this pulse on an inhibitory population $k = i$ is $\phi_{ei}(\mathbf{x}, t) = \mathcal{G}_{ei}(\mathbf{x}, \mathbf{x}_0, t, t_0)$, i.e., the response to the pulse is given by the corresponding \mathcal{G} value. Such \mathcal{G} functions are called “Green’s functions”.

Since the brain is a finite physical object, $\mathcal{G}_{jk}(\mathbf{x}, \mathbf{x}', t, t') \equiv 0$ for $t' \geq t$ and $\mathbf{x}' \notin C$, i.e., future brain activity does not influence earlier one and only connected sources contribute. One also often assumes continuous time invariance: $\mathcal{G}_{jk}(\mathbf{x}, \mathbf{x}', t, t') = \mathcal{G}_{jk}(\mathbf{x}, \mathbf{x}', t - t')$. This means activity propagation depends on conduction delays only. A typical model of this kind contains three factors

$$\mathcal{G}_{jk}(\mathbf{x}', \mathbf{x}, t - t') = \int_0^\infty dv f_{jk}(v | \mathbf{x}, \mathbf{x}') w_{jk}(\mathbf{x}, \mathbf{x}') \delta\left(t - t' - \frac{|\mathbf{x} - \mathbf{x}'|}{v}\right). \quad (11.5)$$

The first factor gives the distribution of conduction velocities v of connecting fibres with $\int_0^\infty dv f_{jk}(v | \mathbf{x}, \mathbf{x}') = 1$. The second factor is the synaptic footprint, which models the strength and distribution of these connections. The last factor calculates the delay by dividing (Euclidean) distance by the conduction velocity.² Only the synaptic footprint $w_{jk}(\mathbf{x}, \mathbf{x}')$ would be modified by synaptic plasticity or neuromodulation, whereas the other two factors express the arrangement and properties of the fibre tracts. If their speed of change is slow compared to propagation, then one can use a delay form and simply change the parameters of the synaptic footprint with time as needed.

Further simplifications come at the price of less biological fidelity. Continuous translation invariance $\mathcal{G}_{jk}(\mathbf{x}, \mathbf{x}', t - t') = \mathcal{G}_{jk}(\mathbf{x} - \mathbf{x}', t - t')$ implies homogeneity of the cortex, i.e., signal transmission then depends only on the *vector distance* between points, not on their location. Clearly this assumption does not hold true for specific connectivity between particular brain areas, yet it can be a reasonable approximation for the dense local “background” connectivity one finds all over the brain. One can further impose continuous rotation invariance: $\mathcal{G}_{jk}(\mathbf{x} - \mathbf{x}', t - t') = \mathcal{G}_{jk}(|\mathbf{x} - \mathbf{x}'|, t - t')$. This establishes isotropy, i.e., independence of fibre direction. Even for background connectivity this does not hold true everywhere in the brain, e.g., primary visual cortex can be modelled by homogeneous but anisotropic connectivity (Robinson 2006; Coombes et al. 2007; Bojak and Liley 2010). Models that are both homogeneous and isotropic are limited to describing qualitative features of brain activity, e.g., the existence of “brain waves” (Robinson et al. 1997; Wu et al. 2008) or drug effects on power spectra (Bojak and Liley 2005).

The “global” theory of Nunez (1974a,b, 1981, 1995), reviewed by Nunez and Srinivasan (2006), ignores the local neural dynamics and focuses on Eq. 11.4:

$$S_e(\mathbf{x}, t) = p(\mathbf{x}, t) + \sum_{j=e,i} q_j \phi_{je}(\mathbf{x}, t), \quad S_i(\mathbf{x}, t) = \sum_{j=e,i} q_j \phi_{ji}(\mathbf{x}, t), \quad (11.6)$$

$$\mathcal{G}_{je}(|\mathbf{x} - \mathbf{x}'|, t - t') = \sum_{n=1}^N \int_0^\infty dv f_n(v) w_n(|\mathbf{x} - \mathbf{x}'|) \delta\left(t - t' - \frac{|\mathbf{x} - \mathbf{x}'|}{v}\right), \quad (11.7)$$

²For realistic cortical geometries Euclidean distance is not a good approximation to axonal fibre length. However, one can adjust the $f_{jk}(v | \mathbf{x}, \mathbf{x}')$ to compensate for geometry.

$$\mathcal{G}_{ji}(|\mathbf{x} - \mathbf{x}'|, t - t') = w_i(|\mathbf{x} - \mathbf{x}'|) \delta(t - t'), \quad w_l(r) \equiv \frac{1}{2} \rho_l \lambda_l e^{-\lambda_l r} \quad (11.8)$$

We see that excitatory and inhibitory ($j, k = e, i$) neuronal populations are being considered. Their output S_k is directly determined by the inputs ϕ_{jk} , where excitatory contributions are weighted positively $q_e > 0$ and inhibitory ones negatively $q_i < 0$. In addition, the excitatory population receives excitatory extracortical innovations p as independent input. Propagation is in delay form, as well as homogeneous and isotropic. Inhibitory connectivity is taken as instantaneous due to a very short characteristic length $1/\lambda_i \simeq 30 \mu\text{m}$. Excitatory connectivity consists of N distinct long range fibre systems.

For a (convoluted) strip of cortex of length $L \simeq 0.5\text{--}1 \text{ m}$, functionally closed by excitatory fibre connections with a single conduction velocity $v_e \simeq 6\text{--}9 \text{ m/s}$, one can estimate that the lowest “standing wave” mode oscillates at frequencies of $f_1 = v_e/L \simeq 6\text{--}18 \text{ Hz}$ consistent with awake EEG (Nunez 1995). An interesting consequence is that larger cortices (larger L) are predicted to oscillate at lower frequencies. It was hence suggested that people with larger heads have lower alpha rhythms (Nunez 1974b; Nunez et al. 1978). An experimental study by Valdés-Hernández et al. (2010) has shown recently that the size of the cortical surface does not correlate with the observed frequency of the alpha rhythm. However, Nunez’ prediction can be rescued simply by assuming that axonal conduction velocity grows in tune with cortical size $v_e \sim L$. This prediction could be tested experimentally, and raises interesting questions about brain development.

In the following we will consider activity propagation with equivalent PDEs. A Fourier transform of Eq. 11.4 for a homogeneous delay form $\mathcal{G}_{jk}(\mathbf{x} - \mathbf{x}', t - t')$ has convolution structure,³ hence

$$\begin{aligned} \phi_{jk}(\mathbf{k}, \omega) &= \int dt \int d\mathbf{x} e^{-i(\omega t + \mathbf{k} \cdot \mathbf{x})} \phi_{jk}(\mathbf{x}, t) = \mathcal{G}_{jk}(\mathbf{k}, \omega) S_j(\mathbf{k}, \omega) \\ &\equiv \frac{Z(\mathbf{k}, \omega)}{P(\mathbf{k}, \omega)} S_j(\mathbf{k}, \omega), \end{aligned} \quad (11.9)$$

For non-zero $P(\mathbf{k}, \omega)$ we can then write

$$\begin{aligned} P \left(-i\nabla, -i\frac{\partial}{\partial t} \right) e^{i\omega t} e^{i\mathbf{k} \cdot \mathbf{x}} \phi_{jk}(\mathbf{k}, \omega) &= Z \left(-i\nabla, -i\frac{\partial}{\partial t} \right) e^{i\omega t} e^{i\mathbf{k} \cdot \mathbf{x}} S_j(\mathbf{k}, \omega) \\ \Rightarrow P \left(-i\nabla, -i\frac{\partial}{\partial t} \right) \phi_{jk}(\mathbf{x}, t) &= Z \left(-i\nabla, -i\frac{\partial}{\partial t} \right) S_j(\mathbf{x}, t), \end{aligned} \quad (11.10)$$

where we have integrated over ω and \mathbf{k} to perform the inverse Fourier transform. Equation 11.10 provides a “mathematically equivalent” PDE formulation wherein the structure of the differential operators P and Z reflects the chosen \mathcal{G} . Why is this

³For \mathcal{G}_{jk} to be homogeneous, the connected region must be a closed (hyper)surface, e.g., a sphere.

rewriting helpful? The connected region C may well encompass the entire brain, and conduction delays can extend to several tens of milliseconds. This makes Eq. 11.4 difficult to evaluate, whereas the PDE evaluation is non-local only in proportion to the order of its differential operators. Using equivalent PDEs can hence greatly simplify analysis and speed up numerical computations.

As mentioned above, Griffith (1963, 1965) was the first to derive the commonly used kind of equivalent PDE, which we will briefly discuss below. However, the PDE approach became popular only through its reintroduction by Jirsa and Haken (1996), and was then investigated further by Robinson et al. (1997) and Liley et al. (2002, 2003). Consider the following

$$\begin{aligned} \hat{\mathcal{G}}(r, \tau) &= \frac{w_0}{2\pi\hat{\sigma}^2} e^{-r/\hat{\sigma}} \cdot \delta\left(\tau - \frac{r}{\hat{v}}\right) \xrightarrow{\mathcal{F}} \hat{\mathcal{G}}(k, \omega) = \frac{w_0 \left(\frac{\hat{\sigma}}{\hat{v}} i\omega + 1\right)}{\left[\left(\frac{\hat{\sigma}}{\hat{v}} i\omega + 1\right)^2 + \hat{\sigma}^2 k^2\right]^{3/2}} \\ \tilde{v} &\equiv \sqrt{\frac{3}{2}} \hat{v}, \quad \tilde{\sigma} \equiv \sqrt{\frac{3}{2}} \hat{\sigma} \quad \Downarrow \quad k^2 \ll \frac{1}{\hat{\sigma}^2} + \frac{\omega^2}{\hat{v}^2} \\ \tilde{\mathcal{G}}(r, \tau) &= \frac{w_0}{2\pi\tilde{\sigma}^2} e^{-\tilde{v}\tau/\tilde{\sigma}} \frac{\Theta\left(\tau - \frac{r}{\tilde{v}}\right)}{\sqrt{\tau^2 - \frac{r^2}{\tilde{v}^2}}} \xleftarrow{\mathcal{F}^{-1}} \tilde{\mathcal{G}}(k, \omega) = \frac{w_0}{\left[\left(\frac{\tilde{\sigma}}{\tilde{v}} i\omega + 1\right)^2 + \tilde{\sigma}^2 k^2\right]} \end{aligned} \quad (11.11)$$

where $r \equiv |\mathbf{x} - \mathbf{x}'|$, $\tau \equiv t - t'$, $k \equiv \sqrt{\mathbf{k} \cdot \mathbf{k}}$ and subscripts are left out for notational simplicity.

Firstly, the homogeneous and isotropic delay ansatz $\hat{\mathcal{G}}(r, \tau)$ propagates activity with a single velocity \hat{v} , and has an exponential decay with characteristic length $\hat{\sigma}$ as the synaptic footprint. Secondly, the Fourier transform $\hat{\mathcal{G}}(k, \omega)$ of this ansatz includes a fractional power $3/2$ that would translate into an infinite series of differential operators, negating any practical advantage of the PDE formulation. Hence thirdly, an expansion $\tilde{\mathcal{G}}(k, \omega)$ for small wavenumbers (i.e., long wavelengths $\lambda = 2\pi/k$) is performed, leading to the following equivalent PDE:

$$\left[\left(\frac{\tilde{\sigma}}{\tilde{v}} \frac{\partial}{\partial t} + 1 \right)^2 - \tilde{\sigma}^2 \nabla^2 \right] \phi(\mathbf{x}, t) = w_0 S(\mathbf{x}, t). \quad (11.12)$$

This “long-wavelength propagator” is an inhomogeneous telegraph equation well suited for analysis and numerics.

However, consider a gamma rhythm $\omega = 2\pi \cdot 38.2 \text{ Hz} \simeq 240.0/\text{s}$ with $\hat{v} = 600 \text{ cm/s}$ and $\hat{\sigma} = 3.33 \text{ cm}$. The “long wavelength expansion” only holds for $k \ll 0.5/\text{cm}$ or $\lambda \gg 13 \text{ cm}$. Even taking cortical folding into account, coherent gamma activity at such scales seems unlikely. It is hence better to consider $\tilde{\mathcal{G}}(k, \omega)$ not as an expansion, but as a new ansatz in its own right, merely “inspired” by the original $\hat{\mathcal{G}}(r, \tau)$. Then fourthly, we can compute its $\tilde{\mathcal{G}}(r, \tau)$, which is easier to interpret in the form of Eq. 11.5:

$$\tilde{w}(r) = \frac{w_0}{2\pi\tilde{\sigma}^2} \mathbf{K}_0\left(\frac{r}{\tilde{\sigma}}\right), \quad \tilde{f}(v|r) = \frac{\tilde{v} \exp(-r/\tilde{\sigma} \cdot \tilde{v}/v)}{v \mathbf{K}_0(r/\tilde{\sigma}) \sqrt{\tilde{v}^2 - v^2}}, \quad (11.13)$$

with the Heaviside step function Θ . The distance-dependent velocity distribution $\tilde{f}(v|r)$ has a complicated distance dependence. However, we can see that the infinitely sharp $\hat{f}(v|r) = \delta(\tilde{v} - v)$ has been softened into a divergence $\sim 1/\sqrt{\tilde{v} - v}$ towards lower velocities $v < \tilde{v}$, whereas no $v > \tilde{v}$ are allowed. Thus most activity will arrive after a delay $\tau = r/\tilde{v}$, but some will arrive more slowly. The synaptic footprint has become a modified Bessel function. Since $\mathbf{K}_0(x) \sim e^{-x}/x$ for large x , this implies a more rapid decay of connectivity with distance.

Most spatially extended simulations use some variant of Eq. 11.12 for activity propagation, because the original ansatz $\hat{\mathcal{G}}(r, \tau)$ in Eq. 11.11 is intuitive and the equivalent PDE Eq. 11.12 is easy to use. Yet we have argued here that their connection is questionable due to the necessary long wavelength expansion. Furthermore, [Bojak and Liley \(2010\)](#) calculated the resulting *marginal* velocity distribution

$$\tilde{f}(v) = \int_0^\infty dr 2\pi r \frac{\tilde{w}(r) \tilde{f}(v|r)}{w_0} = \frac{v \Theta(\tilde{v} - v)}{\tilde{v} \sqrt{\tilde{v}^2 - v^2}}, \quad (11.14)$$

and showed that it is severely incompatible with experimental data on axonal diameter distributions in both rat and human. They proposed new PDEs compatible with the data, in particular the so-called “dispersive propagator” of power $n > 0$:

$$\mathcal{G}_n(r, \tau) = \frac{w_0}{2\pi\sigma_n^2} e^{-r/\sigma_n} \cdot \frac{v_n}{4\sigma_n \Gamma(n)} \left(\frac{v_n \tau}{2\sigma_n}\right)^{n-2} e^{-\frac{1}{2} \left(\frac{\tau - r/v_n}{\sigma_n/v_n}\right)^2} \Theta(\tau), \quad (11.15)$$

$$w_n(r) = \frac{w_0 (r/\sigma_n)^{n-1} \mathbf{K}_{n-1}(r/\sigma_n)}{2^n \pi \Gamma(n) \sigma_n^2}, \quad f_n(v|r) = \frac{e^{-r/\sigma_n \cdot (v_n^2 + v^2)/(2v_n v)}}{2v (v/v_n)^{n-1} \mathbf{K}_{n-1}(r/\sigma_n)}, \quad (11.16)$$

$$\left(\frac{2\sigma_n}{v_n} \frac{\partial}{\partial t} + 1 - \sigma_n^2 \nabla^2\right)^n \phi(\mathbf{x}, t) = w_0 S(\mathbf{x}, t), \quad f_n(v) = \frac{2n v v_n^{2n}}{(v_n^2 + v^2)^{n+1}} \quad (11.17)$$

with the Gamma function Γ . Comparing $\mathcal{G}_n(r, \tau)$ of Eq. 11.15 with $\hat{\mathcal{G}}(r, \tau)$ in Eq. 11.11, we see that the first factor remains unchanged. The second factor of $\mathcal{G}_n(r, \tau)$ turns into a normal distribution of delays $n_\tau(\bar{\tau}, \sigma_\tau^2)$ for $n = 1.5$, with mean $\bar{\tau} = r/v_n$ but *delay-dependent* standard deviation $\sigma_\tau = \sqrt{\tau \sigma_{1.5}/v_{1.5}}$. For longer delays, hence larger distances, the distribution of delays becomes broader. At other n , in particular integer ones providing convenient PDEs, this remains the case qualitatively.

We can furthermore see that for $n = 1$ and $\sigma_n = \tilde{\sigma}$, the synaptic footprints \tilde{w} of Eq. 11.13 and w_n of Eq. 11.16 agree. Furthermore, in that case the equivalent PDEs Eqs. 11.12 and 11.17 agree but for the acceleration term, if $v_n = \tilde{v}$ as well. However, from fits to myelinated fibre data from human corpus callosum, [Bojak and Liley \(2010\)](#) rather suggest $n = 3$ with $v_3 = 14.91$ m/s, and as best comparable

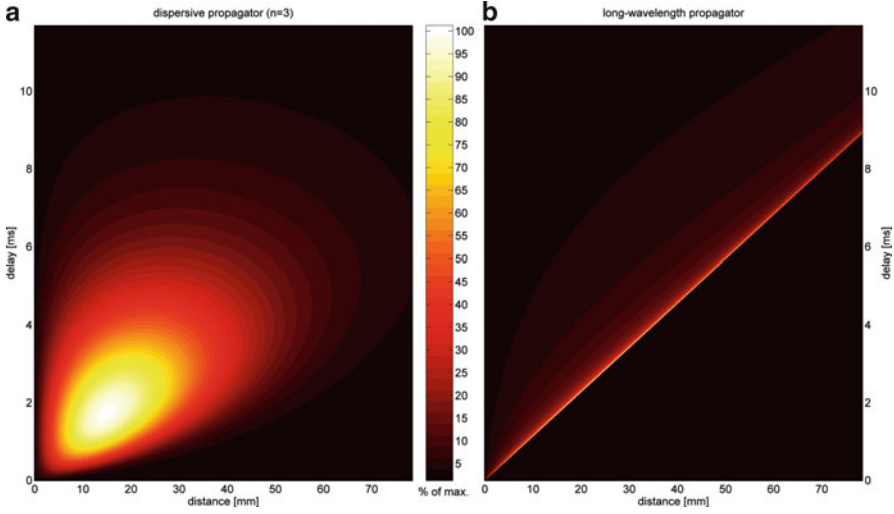


Fig. 11.3 Pulse spreading with the dispersive and long-wavelength propagators. (a) The activation delivery of the dispersive $n = 3$ propagator Eq. 11.17 is shown by integrating its Green's function, cf. Eq. 11.18. (b) Likewise for the long-wavelength propagator Eq. 11.12. Synaptic footprints of both propagators approximate an exponential decay with characteristic length 18 mm. The median conduction velocity of both propagators is 7.601 mm/ms. The colour scale is normed to the respective maximum values as indicated by the central colourbar

values for the long-wavelength propagator $\tilde{v} = 8.782$ m/s and $\tilde{\sigma} = 4.930\sigma_3$. The former leads to the same median velocity 7.601 m/s for both propagators. The latter means that the synaptic footprint of both approximates the same exponential decay, e.g., $\sigma_3 = 0.871$ cm and $\tilde{\sigma} = 4.29$ cm both approximate an exponential decay with a characteristic length of 1.8 cm. Such an effective length scale can be motivated functionally by noting that the coherence of subdural electrode recordings falls to 0.25 at about 2–3 cm (Bullock et al. 1995). Note also the significant difference between the long-wavelength $\tilde{\sigma}$ and the exponential scale, which had been ignored in the literature prior to Bojak and Liley (2010).

In Fig. 11.3 on the left we show the function

$$G_3(i, j) = \int_0^{\Delta\tau} dt \int_0^{\Delta r} dx \frac{1}{w_0} \mathcal{G}_3(i \cdot \Delta r + x, j \cdot \Delta\tau + t) \quad (11.18)$$

with \mathcal{G}_3 of Eq. 11.15 and $i, j = 0, 1, 2, \dots$ specify the discretized values. Note that $\sum_{i=0}^{\infty} \sum_{j=0}^{\infty} G_3(i, j) = 1$, i.e., this shows the spatiotemporal delivery of activity from a single pulse in a properly normed fashion. For comparison we show on the right of Fig. 11.3 the function $\tilde{G}(i, j)$ defined in a like manner using the $\tilde{\mathcal{G}}$ of Eq. 11.11. This method integrates out the discontinuity of $\tilde{\mathcal{G}}$ at $r = v\tau$ and hence facilitates a meaningful comparison of the two propagators. We have used the values mentioned above for comparable median velocity 7.601 mm/ms and characteristic length 18 mm, as well as $\Delta r = 157.1$ μm and $\Delta\tau = 23.41$ μs . The sum of the

shown values of $G_3(i, j)$ is 99.04% but of $\tilde{G}(i, j)$ only 62.51%, i.e., the dispersive propagator has delivered most of the input in the shown spatiotemporal range, the long-wavelength propagator extends further out. We also see the clear difference in overall structure: the long-wavelength propagator is highly concentrated around a line of constant conduction velocity, whereas the dispersive propagator is concentrated in a “blob” around the maximum at $r = 11.6$ mm and $\tau = 2.22$ ms. These different characteristics for example are hypothesised to allow spontaneous pattern formation with the expenditure of less energy (Bojak and Liley 2010).

Finally we briefly consider the earlier work of Wright and Liley (1995, 1996). In contrast to the equivalent PDE approach so far discussed, these authors explicitly discretized the cortical sheet and consequently the activity propagation of Eq. 11.4. A 20 by 20 matrix of neural mass units was used to represent a square cortical sheet, where every unit corresponds to a square with side length 2.79 cm, yielding a total area equivalent to roughly one human hemisphere. Axonal conduction delays were then simply calculated from the Euclidian distance between the centers of the units by dividing with a uniform conduction velocity. Furthermore, the strength of connectivity was determined by a normal distribution with this distance. These assumptions specify two matrices (the strength of connectivity between any two units, as well as their assumed conduction delay), but could easily be replaced with other matrices implying inhomogeneity and anisotropy of the connectivity and complicated conduction velocity profiles with positional dependence.

While this approach is very flexible, it suffers from two fundamental drawbacks: First, the number of possible connections grows with the square of the number of units. Hence increasing the spatial resolution typically comes at a significant computational costs. Second, one needs to keep track of past output from every unit as far back as the maximum conduction delay. If the conduction delays are sizable, then a lot of past values must be kept in memory. It is hence not surprising that in 1995 the chosen grid size was fairly small. While equivalent PDEs numerics employs spatial grids as well, their computation is much less costly. To evaluate Eq. 11.12, minimally one needs to keep track of only two past values of ϕ at every grid point for the time derivatives and consider the four nearest neighbours of every grid point for the Laplacian. Nevertheless, this localized PDE computation instantiates large scale, dense connectivity. However, with ever increasing computational power the greater flexibility of the discretized approach is becoming more important, hence as discussed below this approach is making a comeback in cortical mesh computations.

11.3.4 Realistic Geometry and Connectivity: Robinson et al., Kötter et al., Sotero et al., Bojak et al.

Prior to Robinson et al. (2001), all mean field formulations of cortical activity had posited that any emergent dynamics arises through reverberant interactions between

at least two spatially distributed, functionally differentiated, cortical or thalamic, neuronal populations. However, there exists significant reciprocal connectivity between cortex and the subcortical structure that determines and controls its input, the thalamus. [Robinson et al. \(2001\)](#) have argued that the inclusion of such cortico-thalamic feedback in a bulk or mean-field theory is crucial in order to plausibly model the essential dynamical features of normal (e.g., alpha rhythm) and abnormal (e.g., spike wave epilepsy) EEG activity ([Rodrigues et al. 2006](#); [Breakspear et al. 2006](#)). [van Albada and Robinson \(2009\)](#) have extended the subcortical extent of this model by including interactions between the nuclei of the basal ganglia and cortex and thalamus. We will discuss the influence of subcortical structures on cortical activity further below.

The description of cortical connectivity itself is also far from optimal. While “background connectivity” in cortex ([Liley and Wright 1994](#); [Hellwig 2000](#); [Kaiser et al. 2009](#)) is roughly compatible with assumptions of homogeneity and isotropy, a functionally significant part of the connectivity in the brain is more specific ([Biswal et al. 2010](#)): it connects only particular brain regions to each other and then often over long distances ([Hagmann et al. 2008](#)). While it is possible to simulate anisotropy with PDE approaches ([Robinson 2006](#); [Coombes et al. 2007](#); [Bojak and Liley 2010](#)), this requires simple periodicity to limit computational expense, since the number of necessary PDEs grows with the complexity of the angular profile. Furthermore, the requirement of homogeneity cannot be relaxed, hence this method is only applicable where the anisotropic pattern of connectivity (roughly) repeats across a patch of cortex, like for example in primary visual cortex. The long-range specific connectivity in the brain however does not repeat in this manner.

In order to localize specific cortical connectivity appropriately, one needs anatomically accurate representations of cortex. A first crucial step is hence the extraction of cortical geometry. The imaging technique of choice is structural MRI, which can distinguish different brain tissues on a voxel basis. However, cortical grey matter is basically a layered sheet (2–5 mm thick with 0.2 m² total area), and often a representation as two-dimensional surface is more suitable. Several software packages are available for extracting triangular mesh surfaces from voxels identified with structural MRI, for example, the Civet pipeline ([Kim et al. 2005](#)), see [Fig. 11.4a](#). Often these meshes need some post-processing, e.g., in order to reduce the number of vertices to limit computational cost, see [Fig. 11.4b](#). It should be noted that proper modelling of EEG/MEG requires *oriented* local current dipoles as sources. Their orientation is ultimately dependent on dendritic arborization growing roughly perpendicular to the pial surface. Hence a pure voxel-based approach is insufficient for EEG/MEG signal prediction, and must anyhow be augmented with some estimate of surface normals.

Once one has obtained a cortical surface, the question becomes how to employ it for anatomical mapping. Two methods have been explored: The first is to deform the cortical surface into simpler geometries for computation, e.g., representing each brain hemisphere by a sphere ([Jirsa et al. 2002](#)). The two hemispheres are deformed separately to avoid strong distortions from inflating the compact callosal pathway. However, consider a source point on the simulation sphere, and two target

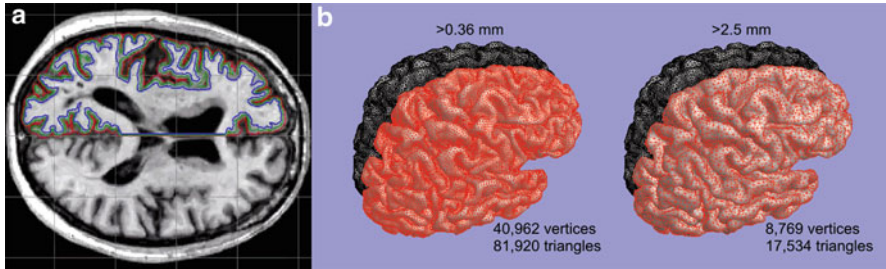


Fig. 11.4 Extraction of a cortical triangular mesh. **(a)** Cross-section of a Civet (Kim et al. 2005) extraction of grey matter interfaces with white matter (*blue*) and cerebrospinal fluid (*red*), respectively, in the *left* hemisphere. Layers can be introduced along vectors connecting corresponding vertices; here a halfway one (*green*) is shown. **(b)** Custom decimation algorithm (Bojak et al. 2011) working on the right hemisphere (*red*) of a Civet cortical mesh. The number of vertices is reduced fivefold while the minimum edge length is increased sevenfold, yet the surface loss is only about 10%

points equidistant along the spherical surface. Given equal conduction velocities, a signal from the source points will reach the target points at the same time. The deformation to the real cortical surface is non-conformal, thus in general the target points will be at different distances from the source point. However, the signal will still arrive at the same time in both, hence the deformation has implicitly made the conduction velocities differ. Such uncontrolled changes to the connectivity are unacceptable beyond qualitative studies. One could ameliorate the situation by introducing compensatory tuning of the conduction velocity. But then one would need to consider conduction between points individually, in effect turning the first method into the second.

The second method works directly on the discretized cortical surface. Then connectivity is instantiated by transferring activity signals from any vertex to each connected vertex, where conduction delays determine the time when the signal is actually released to the receiving vertices. Exactly the same method can be used for connecting grey matter voxels, if one does not extract a cortical surface first (Sotero et al. 2007). This second method is basically the anatomically realistic version of the method introduced by Wright and Liley (1995, 1996), which we have discussed previously. However, as mentioned this method scales badly if connectivity is not sparse. For example, Bojak et al. (2010, 2011) were forced to include about 30 million connections for 17,000 vertices just in order to approximate the dense local connectivity implicit in typical PDE approaches (Bojak and Liley 2010). Furthermore, unlike for networks of spiking neurons, for neural populations typically firing rate information and hence functions continuous in time need to be transferred. This means an event-based approach is impossible, and hence that the necessary parallelization on compute clusters is more difficult.

A series of works involving the late Rolf Kötter (Honey et al. 2007; Ghosh et al. 2008; Deco et al. 2009) established the idea of using tracer connectivity data

from macaque monkey collected in the CoCoMac database (Stephan et al. 2001), by using a “regional map” of brain areas (Kötter and Wanke 2005) across species. See also the extensive review of Deco et al. (2011) focusing on these papers. This may appear odd, since diffusion MRI tractography is readily available (Mori et al. 2005) and there are some interspecies differences that clearly cannot be accounted for in such a mapping, for example concerning areas involved in speech production. However, diffusion MRI is incapable of determining in which direction information flows along reconstructed fibre tracts. This is a major drawback, since it generally makes a significant difference whether a connection is $A \rightarrow B$, $A \leftarrow B$ or $A \leftrightarrow B$. Furthermore, diffusion MRI tends to be biased to short distance connections. Tracer data does not have these drawbacks, which explains its continued popularity in spite of the uncertainties of cross-species mapping (Bojak et al. 2010, 2011).

While modelling is still rapidly improving concerning anatomical fidelity, the basic building blocks are now in place: The geometry of cortical and potentially subcortical structures – as well as skull and scalp for volume conduction for the EEG signal expression – are typically extracted from structural MRI. Gray matter activity is then predicted by assigning neural masses at the chosen resolution level to voxels or mesh vertices. The long-range connectivity of these masses is estimated from diffusion MRI tractography or tracer data. Finally, activity propagation is then performed directly in terms of this discretization, rather than by an equivalent PDE formalism. Nevertheless, the simplicity of the equivalent PDE approach means that we should expect it to remain superior for gaining qualitative understanding or modelling gross changes to the overall brain state, e.g., due to potent drugs.

11.3.5 *Bayesian Inversion: Friston et al., David et al., Moran et al., Daunizeau et al.*

A particular problem encountered in all modelling efforts, including the mean field approach, is to fit the parameters of the model to available experimental data. This is difficult enough in the case of a single model, if it contains a large number of parameters – as is invariably the case for attempts at “biological realism”. The anatomical and physiological constraints on the parameters are then typically weak. Furthermore, as argued in more detail by Liley et al. (2011), projecting parameter space from an “ideal” model to the actual one under investigation generally results in a complicated distribution of the resulting dynamics in parameter space. This may foil straightforward attempts at fitting parameters, potentially requiring novel methods like the “metabifurcation analysis” of Frascaoli et al. (2011) to make any further progress.

Hence it may seem hopeless then to fit entire networks of neural masses to experimental data. However, progress has been made in this direction thanks to the invention of Dynamic Causal Modelling (DCM) by Friston et al. (2003). This original work was intentionally abstract in its assumptions about local dynamics,

positing a bilinear form that connected local neural dynamics and external stimuli. Furthermore, it was targeted at fMRI BOLD rather than EEG or MEG. Yet a crucial novelty was the ability to estimate both parameters of the local bilinear model and of the effective connectivity between several “regions of interest” (ROIs) based on data. To this end advanced Bayesian parameter and model estimation was used, cf. [Friston \(2002\)](#) and [Friston et al. \(2002, 2007\)](#). Briefly, these methods consist in making reasonable assumptions expressed via probability distributions for model parameters, the so-called “prior densities”, followed by an estimate of how likely the available evidence (e.g., experimental data) is given these assumption, the so-called “likelihood”. The probability distributions are then updated according to Bayes’ rule to take the evidence into account, resulting in the so-called “posterior densities”.

Soon after DCM was invented, [David and Friston \(2003\)](#) studied a modification of the mean field model of [Jansen and Rit \(1995\)](#) with two separated ROIs, and later extended it to model event-related responses in EEG and MEG ([David et al. 2005](#)). It was then only natural to combine these efforts with DCM ([David et al. 2006](#); [Kiebel et al. 2006](#)). The fused model included state equations based on the mean field model and observer equations based on an electromagnetic forward model, in effect providing a neurobiologically constrained source reconstruction scheme for the EEG/MEG inverse solution problem. Using this approach, [David et al. \(2006\)](#) were for example able to demonstrate learning-related changes in connectivity for an auditory oddball paradigm. Next [Moran et al. \(2007\)](#) constructed a frequency-domain version of the [Jansen and Rit \(1995\)](#) model, in order to investigate steady-state spectral responses. Again Bayesian parameter estimation ([Moran et al. 2008](#)) and integration with DCM ([Moran et al. 2009](#)) followed. They used this DCM to analyze multi-channel local field potentials from mice. A final crucial step was then taken by [Daunizeau et al. \(2009\)](#): instead of considering sources as point processes, i.e., as equivalent current dipoles, they were distributed over the cortical surface by using a standing wave approximation of the long-wavelength equivalent PDE we have discussed above. Thus one can now say that the entire range of mean field descriptions has been given a DCM-style counterpart suitable for Bayesian inversion.

However, some limitations must be mentioned. Firstly, DCM-style approaches will remain limited to a handful of ROIs for the foreseeable future. The combinatorial explosion of possible connectivity and the per se difficult computation of Bayesian estimates mean that DCMs rapidly become unwieldy when more ROIs are introduced. Secondly, the dependence on prior densities for a specified model structure means that the posterior estimates should not be considered as the ground truth. Thirdly, it seems likely that the present Bayesian inversions gloss over the complexity of the underlying mean field model parameter space to some extent. For the [Jansen and Rit \(1995\)](#) model used throughout the DCM work discussed above, [Spiegler et al. \(2010\)](#) have demonstrated the expected complicated dependence of dynamics on parameter values in the physiological range ([Liley et al. 2011](#)). It hence remains to be seen how comprehensively Bayesian inversion can probe the full dynamical repertoire of mean field models. Nevertheless, the mentioned works represent a pioneering effort in matching mean field models to experimental data.

11.4 Understanding Mesoscopic Brain Activity

Much of what we know about human brain function is derived from non-invasive recording methods that are able to sensitively measure changes in electromagnetic and hemodynamic cortical activity that attend behaviour and cognition. The EEG and MEG measure the spontaneous and evoked electromagnetic activity of large populations of cortical neurons whereas fMRI, based on blood oxygen-level dependent (BOLD) contrast, and near infrared spectroscopy (NIRS) quantify local variations in cerebral blood flow in response to such population activity. Thus the mean field modelling approach, having roughly the same spatiotemporal scales as these recording techniques, is ideally placed to provide physiological explanations of a range of empirical phenomena, some examples of which we discuss below. We believe however that this is just the beginning, agreeing with [Freeman \(1975\)](#) that the field of neurodynamics, of which mean field models are an integral part, “*still can be regarded as a giant sleeping in infancy*”.

11.4.1 EEG Alpha Rhythm: Stochastic, Non-linear, or Both?

The alpha rhythm is arguably the most ubiquitous rhythm seen in scalp recorded EEG. First discovered by [Berger \(1929, 1930\)](#), see also [Gloor \(1969\)](#), and later confirmed by [Adrian and Matthews \(1934\)](#), it has played a central role in phenomenological descriptions of brain electrical activity in cognition and behaviour ever since. While the definition of classical alpha is restricted to 8–13 Hz oscillatory activity recorded over the occiput, which is reactive to eyes opening and closing, activity in the same frequency range can be recorded from multiple cortical areas. However, despite decades of detailed empirical research involving the relationship of this rhythm to cognition, we remain essentially ignorant regarding the mechanisms underlying its genesis and its relevance to brain information processing and function ([Steriade 2005](#)).

To date two broad approaches have emerged for explaining the origin of the alpha rhythm and similar activity. The first approach conceives of alpha as arising from cortical neurons being paced or driven at alpha frequencies: either through the intrinsic oscillatory properties of other cortical neurons ([Llinás 1988](#); [Silva et al. 1991](#)), or through the oscillatory activity of a feed-forward subcortical structure such as the thalamus ([Hughes and Crunelli 2005, 2007](#)). In contrast, the second approach assumes that alpha emerges through the reverberant activity generated by reciprocal interactions of synaptically connected neuronal populations in cortex, and/or through such reciprocal interactions between cortex and thalamus ([Nunez et al. 2001](#)). Two principle lines of evidence have arisen in support of the latter view. Firstly, multichannel MEG ([Williamson and Kaufman 1989](#); [Ciulla et al. 1999](#)) and high density EEG ([Nunez et al. 2001](#)) have revealed that scalp recorded alpha activity arises from a large number or continuum of equivalent current sources

(ECD) in cortex. Secondly, a raft of physiologically plausible computational (Liley et al. 1999a) and theoretical models (Nunez 1981; van Rotterdam et al. 1982; Robinson et al. 1997, 2001; Liley et al. 2002, 2003), reveal that electroencephalographically realistic oscillatory activity can arise from the synaptic interactions between distributed populations of excitatory and inhibitory neurons.

The work of Robinson et al. (2001) suggests that characteristic loop delays in cortico-thalamic and thalamocortical connectivity are responsible for the generation of alpha, and beta (13–30 Hz) electroencephalographic activity. In contrast the work of Liley et al. (2002, 2003) suggests that alpha emerges principally through the reciprocal interactions of populations of inhibitory neurons. In the this case the alpha rhythm can either arise as noise induced perturbations of a cortical system at steady state having an intrinsic alpha resonance or as deterministic (limit cycle or chaotic) oscillation of a far from equilibrium system. Noise driving is more in line with empirical evidence that finds, except for short bursts of subdural and scalp-recorded EEG, that the alpha rhythm is indistinguishable from linearly filtered white noise (Stam et al. 1999; Stam 2005). Other more recent work (Liley et al. 2010) suggests that resting alpha represents a combination of noise-driven and deterministic dynamics and that transitions between the two are not only possible, but are a regular occurrence in resting EEG.

11.4.2 Drug Effects: Anaesthesia, Sedatives, Stimulants

Efforts to maintain biological plausibility in mean field models have enabled the exploration of physiological dynamics during a range of specific brain states. Researchers have therefore focused on how key dynamical attributes are changed during parametric perturbations which attempt to simulate genuine physiological events. As is often customary in neurophysiology, the core of these efforts have focused on changes in excitability through selective modification of inhibitory and excitatory processes. Shifts in brain excitability can occur both through endogenous mechanisms, such as sleep, or pathological conditions, such as seizures (both discussed below) – however, drug induced changes in excitability are another typical starting point. Particular attention has been placed on the modelling of depressant agents like anaesthetics and conversely stimulants such as pro-convulsants (Foster et al. 2008; Liley et al. 2011).

Anaesthesia induced changes are a preferable domain for mean field simulation for several reasons. Firstly, the cellular and molecular targets of anaesthetics are selective and known in some detail. This allows not only meaningful model parameterization, but furthermore enables the use of empirical data to explore the effects of model perturbation within meaningful physiological ranges. Secondly, the effects of anaesthetics at the cellular level produce clear changes in macroscopic scale activity, such as the EEG, in a dose-dependent manner, allowing fairly straightforward experimental validation of the simulations. Finally, the mechanisms by which the cellular or microscopic targets of anaesthetic drugs relates to the

observed macroscopic effects recorded by the EEG are far less clear, promoting the use of mesoscopic methods to help link these physical scales and elucidate the intriguing processes occurring during the transition to unconsciousness.

Generally, anaesthetics, as well as sedatives (e.g. benzodiazepines), produce their depressant effects by targeting inhibitory neurotransmission through enhancement of GABA_A receptor function. By potentiating GABA_A receptor based IPSPs, anaesthetics can progressively suppress neural firing. Less obviously, one also finds a slowing of the EEG that appears in the time domain as a shift from low amplitude desynchronised EEG to large amplitude slow oscillations, and in the frequency domain as a shift from peaked alpha power spectra to ones dominated by the delta band (0–4 Hz). This overall cortical slowing of activity has been successfully modelled by a number of investigators, however explanations for the spectral changes which occur during the *transition* between wakeful rest and deep anaesthesia are somewhat more controversial. During the induction of anaesthesia, the EEG in humans (Kuizenga et al. 1998) and other species (Dutta et al. 1997) show a rise in power prior to the onset of slow wave activity, which approximately coincides with the loss of consciousness (LOC). Typically referred to as the *biphasic response*, studies have shown that a variety of anaesthetic agents produce transient increases in EEG activity in the frequency ranges more associated with alertness and arousal during both induction and emergence (Kuizenga et al. 1998, 2001; Feshchenko et al. 2004). Interestingly, because such effects may be more pronounced during emergence than induction, a number of modelling approaches have taken this as an explanatory predicate in simulations of the biphasic response and its hypothesised hysteresis (system dependence on prior history).

Steyn-Ross et al. (1999, 2004) modelled the biphasic response as a first-order phase transition using the mean field cortical model of Liley et al. (1999b). By selectively modifying the inhibitory neurotransmitter decay rate constant, they found three stages of analytic equilibrium for changes in the level of anaesthesia defined by λ , a scaling-factor representing the fractional change in IPSP duration from the non-anaesthetized state. These stages were termed (1) “coma” (high anaesthesia $\lambda > 1.53$); (2) “awake” (low/no anaesthesia $\lambda = 1$), and (3) “seizure” (retracted inhibition $\lambda < 0.3$). During the transitions between these states estimated EEG spectra were shown to display a clear biphasic response. It was therefore posited that the biphasic response was coincident with the transition between stable states, from (2) to (1) or (3), via a saddle node bifurcation, reflecting a phase transition in the mean soma membrane potential. While this phase transition theory was an innovative and appealing integration of the biphasic response and the loss of consciousness during anaesthesia, the model depended upon neural firing rate parameters outside physiological ranges with “awake” power spectra devoid of any resting alpha activity.

Subsequent work by Bojak and Liley (2005) showed that biphasic phenomena can still be simulated without the occurrence of a phase transition and within plausible firing rate ranges. They used mean field model parameter sets restricted by physiological limits with proper resting state behaviour, and realistically modelled

the effects of the anaesthetic agent isoflurane by allowing independent modifications of IPSP amplitude, rise and decay times based on empirical data. The simulated biphasic response was then not coincident with rapid shifts in firing rates, but rather consistent with empirical observations of progressive dose dependent spike suppression. [Bojak and Liley \(2005\)](#) were also pioneering in the mean field context by using a large number of base parameter sets to gain an understanding of the robustness of the predictions under conditions of typical biological variability. This approach has become popular in the field of individual neuron models ([Marder and Taylor 2011](#)). [Molae-Ardekani et al. \(2007\)](#) later showed that the application of a slow adaptive function for the modelling of firing rates was capable of both simulating biphasic spectral activity and relating the slowing of firing rates to the well know occurrence of up/down state firing modes during anaesthesia and slow wave sleep. More recently [Hutt and Longtin \(2010\)](#) have sought to connect both descriptions of biphasic activity. For a simplified model they were able to derive conditions under which the anaesthetic agent propofol causes the biphasic effect either by a phase transition or without.

The possibility of linking the biphasic response of cortical populations with the LOC is a fascinating area for future computational research. Yet it remains unclear if the biphasic changes in EEG spectral power are even causally linked to LOC or whether these two events arise independently in response to pharmacological action. For example, empirical and theoretical work has shown that benzodiazepines such as diazepam and alprazolam, which also selectively target GABA_A receptors, can produce arousal responses in EEG spectral power producing acceleration of peak alpha frequency into the low beta range ([Liley et al. 2003b](#)). This “beta buzz” is not greatly different from that produced by alcohol, a GABA_A agonist also. Therefore the occurrence of this form of biphasic response is interpreted as being reflective of low dose anaesthesia and not as a marker of a specific dynamical transition, for this effect may extended over a period far greater than the interval associated with the loss of consciousness. Such effects can be informed by the observed sensitivity of inhibitory synapses and the time delays associated with their reverberant activity ([Liley et al. 2003b](#)): enhancement of inhibitory–inhibitory coupling through GABA agonists will strengthen, and therefore shorten, the interactions of this population shifting alpha power to higher frequencies ([Liley et al. 2002, 2003](#)).

There has been little application of mean field modelling to understanding the macroscopic action of stimulants, because the involved pharmacological and physiological mechanisms are less straightforward to include in the established formulations. Interestingly, the study by [Rowe et al. \(2005\)](#) concerning the action of stimulants in attention deficit hyperactivity disorder points to yet another *inhibitory* effect, namely decreased firing activity in the locus coeruleus. The authors speculate that more generally stimulants could act to suppress the activity of the thalamic reticular nucleus, thereby increasing thalamocortical and synaptic activity. If true, then once more one would find that inhibitory control is a key locus for the control of brain dynamics.

11.4.3 Cognitive States: Sleep, Rest, Memory, Attention

Following progress in the mean field modelling of anaesthesia, a number of researchers have gone on to theoretically account for human sleep cycles and a range of other cognitive phenomena. Some investigators have extended existing mean field models to incorporate further differentiated neural populations (typically subcortical nuclei), whereas others have focused on purely parametric perturbation of a putative (noise driven) cortex alone. Regarding the modelling of sleep cycles, [Steyn-Ross et al. \(2005a\)](#) have explored the latter approach by modelling the role somnogenic (sleep promoting) factors have in modulating cortical arousal. Conversely [Phillips and Robinson \(2007\)](#) have explored the former approach by applying mean field theory to simulate the modulatory effects of ascending brain stem projection systems. We will discuss each of these approaches in turn.

[Steyn-Ross et al. \(2005a\)](#) model sleep states with particular attention to the transition between slow wave sleep (SWS) and rapid eye movement (REM) phases. In this approach the authors employ a macrocolumn whose characteristic time scales have been greatly increased from their standard parameter values in order to better incorporate the time courses associated with the ultradian human sleep cycle (≈ 90 min). Subsequently, the transition between SWS and REM states are parameterized as arising from the differential modulation of the basal K^+ leak currents by the somnogenic adenosine ($\uparrow K^+$ leak) and activating acetylcholine (ACh; $\downarrow K^+$ leak). In combination, these effects were best captured through modification of the coupling strength at excitatory synapses with a factor λ_{ACh} scaling the excitatory synaptic gain. Similar to their work in anaesthesia, this parameterization produced a first-order phase transition, typified by a rapid shift from coherent slow firing (SWS) to a classical desynchronized high firing state. Approaching the point of transition between these two states was characterized by increasing coherent frequency power in progressively slower frequencies. This system also supports the occurrence of K-complexes (transient spike-like waves), which typically occur during sub-arousal stimulation (e.g., auditory) during REM sleep. [Wilson et al. \(2006\)](#), explored the response of cortex to such transient *kicks* in input. It was found that depending on system state (SWS or REM), transient shifts in membrane potential cause different spatiotemporal oscillations.

Finally, these authors have also explored the capacity of putative Hebbian learning in such systems in relation to memory consolidation during sleep. [Steyn-Ross et al. \(2005b\)](#) postulate a mechanism for memory erasure or unlearning during the suppressive dynamics occurring during the approach to the SWS-REM transition. Then SWS oscillations become more coherent and expanded in phase-space, producing a state preferentially enhancing inhibitory synaptic weights, after which the REM sleep will reset synaptic weights back to a state capable of learning. [Wilson et al. \(2007\)](#) extended their model to allow estimation of synaptic weight distribution and other statistical attributes, which help to link Hebbian network descriptions with mesoscopic columnar field models.

In contrast to the previous approach, [Phillips and Robinson \(2007\)](#) have included the cortically ascending projections of the various brain stem nuclei which are involved in mediating arousal and therefore the sleep-wake cycle. This ascending arousal system has cortical projections which terminate diffusely across the cerebrum. [Phillips and Robinson \(2007\)](#) model this group of nuclei by defining a monoamine group (MA) and a ACh group, both of which receive driving (e.g., circadian) inputs from the ventrolateral preoptic area (VLPO; hypothalamus). Since the interaction of the defined MA and ACh groups reflect nuclei whose reciprocal action is thought to control SWS-REM switching, [Phillips and Robinson \(2007\)](#) focus only on interactions between the VLPO and MA groups, while setting the ACh group constant. Thus they focus on the transition between waking and sleeping states and not the ultradian sleep cycle (i.e., sleep stages). The mutual inhibition between the MA group (wake promoting) and the VLPO (sleep promoting) are parametrically explored as putative sleep-wake cycling. By modulating the driving input, they observed clear changes in the mean soma membrane potential of the MA group, such that wake-sleep transitions occur as a saddle node bifurcation at several driving values which produces a hysteresis in the return from sleep to waking states. This hysteresis produces a zone wherein the transition between awake and sleep states is more easily achieved and more sensitive to noise. This unstable transition is suggested by the authors to dynamically underpin the phenomenon of narcolepsy.

Attempts to model learning process through the modification of synaptic properties represents one example of how mean field theories may begin to make contact with cognition and cognitive systems. However, it remains difficult to meaningfully capture the dynamics of cognitive activity with these simple biological models. Currently the focus is on explaining activity patterns and to use data-driven approaches to help identify physiological parameters that sensitively control neuronal population dynamics. For example, [Steyn-Ross et al. \(2009\)](#) have explored the utility of mean field models to capture differing dynamical properties associated with activity patterns during resting and cognitive states. In brief, this work suggests that the ongoing activity of the brain may be the result of spatiotemporal instabilities, with idling activity slowly oscillating (1 Hz) around a rest state that can be perturbed into an active cognitive state defined by faster (40 Hz) activity. Such slow oscillations may relate to those observed during resting state neuroimaging ([Steyn-Ross et al. 2009, 2011](#)) – the so called “*default mode*” ([Raichle et al. 2001](#)). Concrete studies of cognitive action have also been performed, in particular of (visual) attention ([Deco and Rolls 2005; Mavritsaki et al. 2011](#)). Interestingly in these cases, hybrid descriptions in terms of both spiking neurons and mean field models were employed, which interacted consistently with each other by construction ([Brunel and Wang 2001](#)). It is likely that such hybrid approaches will become more common in the future.

11.4.4 *Special Dynamics: Metastability, Gamma Synchrony, Epilepsy*

Although early attempts to dynamically describe brain function sought to prescribe explicit attractor dynamics to neural activity, more recent thinking focuses on transitory non-equilibrium behaviour (Rabinovich et al. 2008a). Neuronal population dynamics are conceived as evolving transiently, rarely reaching stability. On this basis a number of authors have opted to describe this type of dynamical regime as metastability (Kelso 1995; Friston 1997; Bressler and Kelso 2001; Freeman and Holmes 2005; Rabinovich et al. 2008b). Common to many of these descriptions is an ongoing occurrence of transitory neural events, or state transitions, which define the flexibility of cognitive and sensori-motor function. Some dynamical examples include the chaotic itinerancy of Tsuda (2001), in which neural dynamics transit in a chaotic motion through unique Milnor attractors, or the liquid-state machine of Rabinovich et al. (2008a), where a more global stable heteroclinic channel is comprised of successive local saddle states. More specific neurodynamical approaches include the work of Kelso (1995), Friston (2000) and Freeman and Holmes (2005).

The idea that the brain activity switches between qualitatively different states is reflected in the dynamical behaviour of many mean field model formulations. For this reason it has been conjectured that mean field models may offer a suitable explanatory framework in which to understand the genesis and evolution of epileptic activity (Wendling et al. 2000; Robinson et al. 2002; Lopes da Silva et al. 2003; Suffczynski et al. 2005; Kramer et al. 2005; Liley and Bojak 2005; Breakspear et al. 2006; Marten et al. 2009; Molaee-Ardekani et al. 2010) as well as the formation of coherent mesoscopic gamma band activity (Wright 1997; Rennie et al. 2000; Robinson 2006; Bojak and Liley 2007). What relates these two topics is that such dynamics are typically conceived as limit cycle (or chaotic) behaviour to which the brain transits from a regular state under certain conditions, e.g., the change of some physiological parameter. The difference between epilepsy and gamma synchrony is then mainly related to the dominant frequency of these “special” dynamics. That the dominant frequency typically can be adjusted with some model parameter suggests that these phenomena may indeed be physiologically related.

However, a general caveat applies to such studies: it is often comparatively easy to obtain activity that resembles epilepsy or coherent gamma oscillations from complicated (mean field) models. That per se should hence not count as a success of the model. Rather, it is precisely the mechanistic explanation of the transit from regular to special dynamics which then becomes a hallmark of biological fidelity. For example, Liley and Bojak (2005) showed that seizure-inducing properties of some general anaesthetic agents could be reproduced with the Liley mean field model, rather than just that the model supported seizure-like limit cycles. At the very least the switching mechanism should be post hoc interpreted, like the emergence of large scale gamma synchrony in terms of changes in presynaptic thalamocortical input (Bojak and Liley 2007).

11.4.5 Beyond Electrical Activity: fMRI BOLD and Multimodal Integration

The EEG's continued popularity in research and clinical practice (Niedermeyer and Lopes da Silva 2005) is largely due to its excellent time resolution, which allows for example the tracking of evoked potentials (Regan 1989; Rennie et al. 2002). EEG taken with a large number of electrodes and MEG can provide data of brain activity with comparatively high spatial resolution in the centimetre range. However, due to its millimetre resolution fMRI BOLD has taken over as the de facto standard for researching cognition (Norris 2006; Matthews et al. 2006), in spite of weak temporal resolution and uncertainties concerning its genesis (Logothetis 2008). The rapidly growing field of multimodal imaging (Stufflebeam and Rosen 2007; Shibasaki 2008; Mulert et al. 2008; Blinowska et al. 2009; Freeman et al. 2009) also promises to combine the excellent temporal resolution of EEG with the good spatial resolution of fMRI BOLD. This combination is particularly attractive because it is possible to record EEG and fMRI BOLD simultaneously (Laufs et al. 2008), which avoids all the issues of brain state dependence that arise in combining data sets recorded at different times (or even from different people). Furthermore, the relation of fMRI resting state networks to EEG cortical microstates (Britz et al. 2010; Musso et al. 2010) suggests close dynamical links between data recorded with these modalities.

Therefore it is of obvious interest to extend the mean field formalism first to the description of fMRI BOLD, and then to the prediction of simultaneous EEG/fMRI. The first issue to confront is the addition of appropriate hemodynamics. Almost all mean field modellers have adopted the so-called "Balloon-Windkessel" hemodynamic model in the form introduced by Friston et al. (2000, 2003) based on prior work by Buxton and Frank (1997), Buxton et al. (1998) and Mandeville et al. (1999). The main reason is that this model merely adds four ordinary differential equations (ODEs) to the equations, with specified (prior) parameter values. The Balloon-Windkessel model will predict the BOLD contrast based on neural activity innovations, making it most suited for task paradigms. It is somewhat less suited for resting state activity (Bojak et al. 2010, 2011), a point that will require scrutiny in future. Note that these equations are local, hence in a large scale model comprising many neural masses or in a continuous formulation discretized for numerical computation, the ODE systems must be evaluated at every unit. Furthermore, the question arises what neural activity to use as input for the Balloon-Windkessel hemodynamics, or in other terms, how the neurovascular coupling is modelled. In the works we will describe below, a bewildering variety of models have been used, though conceptually they reduce to either total synaptic activity, glutamate release or energy consumption. We believe that this confusion reflects our limited knowledge about the genesis of the BOLD signal and refrain here from commenting further on this issue. Suffice to say that all current modelling efforts must be considered speculative concerning the fMRI signal generation.

We have already mentioned the works using CoCoMac connectivity (Honey et al. 2007; Ghosh et al. 2008; Deco et al. 2009), recently reviewed by Deco et al.

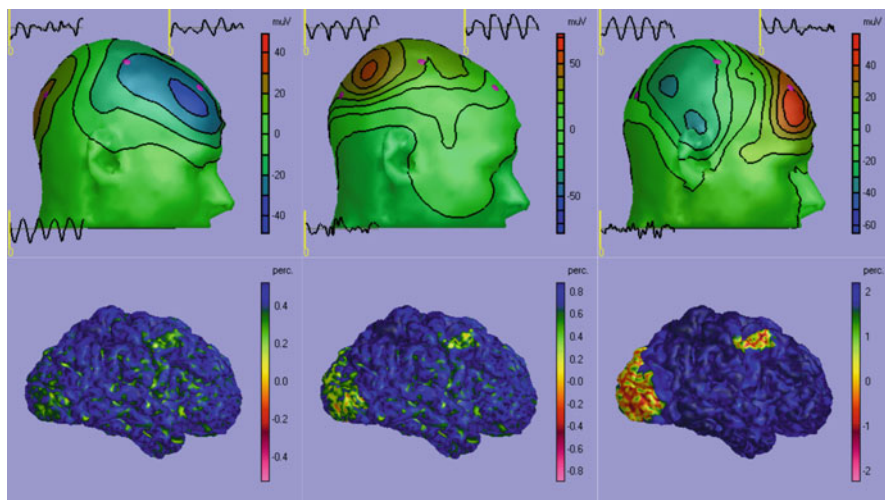


Fig. 11.5 Simultaneous EEG/fMRI BOLD prediction. The *top* row shows snapshots of EEG scalp potentials, as well as EEG time traces from three electrodes (*purple*). The *bottom* row shows corresponding fMRI BOLD predictions (Bojak et al. 2010, 2011). Columns from *left* to *right* show results for specific connectivity at 60%, 85%, and 90% strength relative to that of local (“background”) connectivity. Scales vary between panels and are indicated by colourbars. A clear jump in fMRI BOLD contrast occurs for increasing the strength from 85% to 90%

(2011). They all provide multimodal EEG and fMRI predictions, whereas the related paper by Honey et al. (2009) used diffusion MR tractography and predicted only fMRI signals. The focus of these works is on resting state oscillations and the so-called “default mode network” (Raichle et al. 2001). General experimentally observed features were reproduced; however, Honey et al. (2009) raises questions about the dependence of such dynamics on the cortical parcellation. Babajani et al. (2005), Babajani and Soltaninan-Zadeh (2006) and Babajani-Feremi et al. (2008) convincingly fit both MEG and fMRI BOLD data arising from an auditory task with a single underlying model. Recently Babajani-Feremi and Soltaninan-Zadeh (2010) also extended the electrocortical part of this model to multiple areas. Riera et al. (2005, 2006, 2007) have successfully fit simultaneous EEG/fMRI data in visual and auditory tasks, though their focus was more on the technical development of inversion and neurovascular coupling models. Sotero et al. (2007), Sotero and Trujillo-Barreto (2008) and Valdes-Sosa et al. (2009) pioneered highly resolved descriptions of the brain geometry and obtained intriguing results on “alpha blocking” and BOLD-alpha rhythm (anti-)correlation, respectively. Deneux and Faugeras (2010) studied in-depth the extent to which simultaneous EEG/fMRI can extract information beyond the use of single modalities. To this end they developed Kalman filters and smoothers for the inverse problem. Finally, Bojak et al. (2010, 2011) show that minor changes in the implemented effective connectivity can lead to drastic changes in the simulated dynamics, see Fig. 11.5.

11.5 Conclusions

Mesoscopic and coherent neural activity is important for three distinct but intimately related reasons. Firstly, the brain appears to have multiple anatomical structures that bind together larger groups of neurons in a “columnar” fashion and so parcellate cortex into units. A corresponding degree of functional coherence can be assumed to follow, and to some extent has been shown to exist. Secondly, non-invasive neuroimaging is at least for the time being limited to a spatial resolution of larger than 1 mm for fMRI, and worse for the other modalities, e.g., in the centimetre range for EEG. Furthermore, coherent microscopic activity dominates such macroscopic signals for statistical reasons. Thirdly, theoretical descriptions at the level of individual neurons (or smaller) scale badly in computational costs for a variety of reasons. Yet even if large scale simulations of this kind increasingly become possible in a computational sense, they remain questionable for the foreseeable future: one cannot expect to ever gather enough data to fully specify any sizable part of the brain, in particular not a single actual structure, rather than some statistics about a large number of similar structures.

Bulk models of neural activity try to describe mesoscopic activity directly, eschewing a description in terms of enumerable microscopic units. Yet they typically retain selected “microscopic features” that are salient for the description of the phenomena of interest. Thus for example if it is known that some drugs affects the PSPs of individual neurons, then it is advantageous if the bulk approach employed contains a PSP description that can be matched to this “microscopic” knowledge. The simplest bulk models consider only the mean (i.e., first moment) properties of neuronal ensembles. Here the connection to the microscopic world is generally direct, replacing a microscopic quantity by its mesoscopic mean. We have described in great detail how these models developed historically, and what sort of brain activity they are able to describe successfully. We will not repeat our observations here. Suffice to say that mathematical and computational progress has been good and seems to be accelerating still, and a great number of applications have been found already.

To this clear success story we have told in the preceding pages we now wish to add a more critical perspective and some caveats. Firstly, the microscopic-mesoscopic connection remains fairly ill-defined. It is unclear to what extent a population description can and should be made “consistent” with existing single neurons models: the brain consists of much more than just neurons and bulk approaches should subsume these non-neural contributions in their “effective equations”. The necessity to maintain salient microscopic features however means that the bulk descriptions often closely resemble single neuron models after all, to allow direct mapping of known effects. Yet it is unclear to what extent this similarity of form remains justified for an effective description that includes other elements. Indeed, as comparing Newton’s equations with the ideal gas law suggests, it is far from certain that the best mesoscopic description of even a purely neuronal and homogeneous population would resemble the individual neuron model at all.

A certain amount of “hand-waving” seems to be required at the moment to motivate all bulk models. We suggest that much future work is required to clarify the situation.

Secondly, applications of bulk models have yet to deliver an insight of such obvious neuroscientific or medical impact that their future importance is established beyond reasonable doubt. In other words, this field still requires an universally accepted breakthrough. An important limiting factor in this regard is the lack of information intrinsically associated with the predicted activity. While the single neuron modeller can dream of cracking the “spike code” of information processing in the brain, it is currently not obvious what bulk activity *means*. We need to learn better how to associate computation with bulk activity, how to assign meaning to the energetic flows that are presently being modelled. There seem to be two ways forward here: On one hand one can try to elucidate further the effect of coherent group activity on single neurons, and thus establish a meaning for the mesoscopic activity in terms of whatever meaning single neuron activity may have. On the other hand one can try to connect to the more abstract models of psychology and psychophysics. Their natural “neural basis” may very well be found in bulk approaches. It seems to us that both paths to greater impact must now be pursued vigorously.

Thirdly, at the cutting edge of technical development, bulk approaches are meeting challenges that are rather reminiscent of the problems single neuron modellers face. If one attempts to describe the entire brain at mesoscopic resolution in the millimetre range, one ends up with about the same number of mesoscopic units (many tens of thousands) as large scale single neuron simulations. Thus the same issues of computational cost, combinatorial explosion of connectivity and experimental indeterminacy arise. We cannot, and likely will not ever, simulate *this* brain here and now even at a mesoscopic level, just as attempts to simulate *this* macrocolumn here and now are doomed to failure. What we need to work out is hence the appropriate level of detail: where can and should we introduce individual features, where should we stick to stereotypical and qualitative descriptions. Furthermore, the issue of fitting to experimental data the many parameters of a large number of functional units in a complicated network remains unresolved, and limits progress at both the mesoscopic and microscopic level. We will likely need the help from experts in the statistical field to break this gridlock.

However, such technical challenge also provide chances for future growth, and the need for bulk approaches becomes increasingly clear. We would like to particularly encourage our experimental colleagues to consider the mesoscopic level of investigation as a field with enormous growth potential. Mesoscopic theory is now getting to a level where it can speak to experimental recordings from multi-electrode arrays recording LFPs in stimulated slice preparations all the way to complex task paradigms tracked with fMRI BOLD. Modern experimental technologies can go in many ways beyond the patch-clamping of a single neuron, and most of those involve the consideration of the collective activity of neurons. The marriage of experiment and theory has not always been easy in the neurosciences, but there is a

clear convergence of interest here concerning the activity of many neurons working together. As neuroscientists we should respond to this opportunity by working together as well.

References

- Aboitiz F, Scheibel AB, Fisher RS, Zaidel E (1992a) Fiber composition of the human corpus callosum. *Brain Res* 598:143–153
- Aboitiz F, Scheibel AB, Fisher RS, Zaidel E (1992b) Individual differences in brain asymmetries and fiber composition in the human corpus callosum. *Brain Res* 598:154–161
- Adrian ED, Matthews BHC (1934) The Berger rhythm, potential changes from the occipital lobe in man. *Brain* 57:355–385
- Amari SI (1975) Homogeneous nets of neuron-like elements. *Biol Cybern* 17:211–220
- Amari SI (1977) Dynamics of pattern formation in lateral-inhibition type neural fields. *Biol Cybern* 27:77–87
- Araque A, Navarrete M (2010) Glial cells in neuronal network function. *Philos Trans R Soc B* 365:2375–2381
- Azevedo FAC, Carvalho LRB, Grinberg LT, Farfel JM, Ferretti REL, Leite REP, Jacob Filho W, Lent R, Herculano-Houzel S (2009) Equal numbers of neuronal and nonneuronal cells make the human brain an isometrically scaled-up primate brain. *J Comp Neurol* 513:532–541
- Babajani A, Soltaninan-Zadeh H (2006) Integrated MEG/EEG and fMRI model based on neural masses. *IEEE Trans Biomed Eng* 53:1794–1801
- Babajani A, Nekooei MH, Soltaninan-Zadeh H (2005) Integrated MEG and fMRI model: synthesis and analysis. *Brain Topogr* 18:101–113
- Babajani-Feremi A, Soltaninan-Zadeh H (2010) Multi-area neural mass modeling of EEG and MEG signals. *NeuroImage* 52:793–811
- Babajani-Feremi A, Soltaninan-Zadeh H, Moran JE (2008) Integrated MEG/fMRI model validated using real auditory data. *Brain Topogr* 21:61–74
- Ben Achour S, Pascual O (2010) Glia: the many ways to modulate synaptic plasticity. *Neurochem Int* 57:440–445
- Berger H (1929) Über das Elektrenkephalogramm des Menschen. *Arch Psychiatr Nervenkr* 87:527–570
- Berger H (1930) Über das Elektrenkephalogramm des Menschen. Zweite Mitteilung. *J Psychol Neurol* 40:160–179
- Beurle RL (1956) Properties of a mass of cells capable of regenerating pulses. *Philos Trans R Soc B* 240:55–94
- Biswal BB, Mennes M, Zuo XN, Gohel S, Kelly C, Smith SM, Beckmann CF, Adelstein JS, Buckner RL, Colcombe S, Dogonowski AM, Ernst M, Fair D, Hampson M, Hoptman MJ, Hyde JS, Kiviniemi VJ, Kötter R, Li SJ, Lin CP, Lowe MJ, Mackay C, Madden DJ, Madsen KH, Margulies DS, Mayberg HS, McMahon K, Monk CS, Mostofsky SH, Nagel BJ, Pekar JJ, Peltier SJ, Petersen SE, Riedel V, Rombouts SAR, Rypma B, Schlaggar BL, Schmidt S, Seidler RD, Siegle GJ, Sorg C, Teng GJ, Veijola J, Villringer A, Walter M, Wang L, Weng XC, Whitfield-Gabrieli S, Williamson P, Windischberger C, Zang YF, Zhang HY, Castellanos FX, Milham MP (2010) Toward discovery science of human brain function. *Proc Natl Acad Sci USA* 107:4734–4739
- Blinowska K, Müller-Putz G, Kaiser V, Astolfi L, Vanderperren K, Van Huffel S, Lemieux L (2009) Multimodal imaging of human brain activity: rational, biophysical aspects and modes of integration. *Comput Intell Neurosci* 2009:813607
- Bojak I, Liley DTJ (2005) Modeling the effects of anesthesia on the electroencephalogram. *Phys Rev E* 71:041902

- Bojak I, Liley DTJ (2007) Self-organized 40 hz synchronization in a physiological theory of EEG. *Neurocomputing* 70:2085–2090
- Bojak I, Liley DTJ (2010) Axonal velocity distributions in neural field equations. *PLoS Comput Biol* 6:e1000653
- Bojak I, Oostendorp TF, Reid AT, Kötter R (2010) Connecting mean field models of neural activity to EEG and fMRI data. *Brain Topogr* 23:139–149
- Bojak I, Oostendorp TF, Reid AT, Kötter R (2011) Towards a model-based integration of co-registered EEG/fMRI data with realistic neural population meshes. *Philos Trans R Soc A* 369:3785–3801
- Braitenberg V, Schüz A (1998) *Cortex: statistics and geometry of neuronal connectivity*, 2nd edn. Springer, Berlin
- Branco TP, Staras K (2009) The probability of neurotransmitter release: variability and feedback control at single synapses. *Nat Rev Neurosci* 10:373–383
- Breakspear M, Roberts JAG, Terry JR, Rodrigues S, Mahant N, Robinson PA (2006) A unifying explanation of primary generalized seizures through nonlinear brain modeling and bifurcation analysis. *Cereb Cortex* 16:1296–1313
- Bressler SL, Kelso JAS (2001) Cortical coordination dynamics and cognition. *Trends Cogn Sci* 5:26–36
- Britz J, Van De Ville D, Michel CM (2010) BOLD correlates of EEG topography reveal rapid resting-state network dynamics. *NeuroImage* 52:1162–1170
- Brodmann K, Garey LJ (2006) *Brodmann's localisation in the cerebral cortex: the principles of comparative localisation in the cerebral cortex based on cytoarchitectonics – translated with editorial notes and an introduction*, 3rd edn. Springer, New York
- Brunel N, Wang XJ (2001) Effects of neuromodulation in a cortical network model of object working memory dominated by recurrent inhibition. *J Comput Neurosci* 11:63–85
- Buice MA, Cowan JD, Chow CC (2010) Systematic fluctuation expansion for neural network activity equations. *Neural Comput* 22:377–426
- Bullock TH, McClune MC, Achimowicz JZ, Iragui-Madoz VJ, Duckrow RB, Spencer SS (1995) EEG coherence has structure in the millimeter domain: subdural and hippocampal recordings from epileptic patients. *Electroencephalogr Clin Neurophysiol* 95:161–177
- Buxhoeveden DP, Casanova MF (2002) The minicolumn and evolution of the brain. *Brain Behav Evol* 60:125–151
- Buxton RB, Frank LR (1997) A model for the coupling between cerebral blood flow and oxygen metabolism during neural stimulation. *J Cereb Blood Flow Metab* 17:64–72
- Buxton RB, Wong ECC, Frank LR (1998) Dynamics of blood flow and oxygenation changes during brain activation: the balloon model. *Magn Reson Med* 39:855–864
- Ciulla C, Takeda T, Endo H (1999) MEG characterization of spontaneous alpha rhythm in the human brain. *Brain Topogr* 11:211–222
- Contreras D (2004) Electrophysiological classes of neocortical neurons. *Neural Netw* 17:633–646
- Coombes S (2005) Waves, bumps, and patterns in neural field theories. *Biol Cybern* 93:91–108
- Coombes S (2010) Large-scale neural dynamics: simple and complex. *NeuroImage* 52:731–739
- Coombes S, Venkov NA, Shiau LJ, Bojak I, Liley DTJ, Laing CR (2007) Modeling electrocortical activity through improved local approximations of integral neural field equations. *Phys Rev E* 76:051901
- Daunizeau J, Kiebel SJ, Friston KJ (2009) Dynamic causal modelling of distributed electromagnetic responses. *NeuroImage* 47:590–601
- David O, Friston KJ (2003) A neural mass model for MEG/EEG: coupling and neuronal dynamics. *NeuroImage* 20:1743–1755
- David O, Harrison LM, Friston KJ (2005) Modelling event-related responses in the brain. *NeuroImage* 25:756–770
- David O, Kiebel SJ, Harrison LM, Mattout J, Kilner JM, Friston KJ (2006) Dynamic causal modeling of evoked responses in EEG and MEG. *NeuroImage* 30:1255–1272
- Deco GR, Rolls ET (2005) Neurodynamics of biased competition and cooperation for attention: a model with spiking neurons. *J Neurophysiol* 94:295–313

- Deco GR, Jirsa VK, Robinson PA, Breakspear M, Friston KJ (2008) The dynamic brain: from spiking neurons to neural masses and cortical fields. *PLoS Comput Biol* 4:e1000092
- Deco GR, Jirsa VK, McIntosh AR, Sporns O, Kötter R (2009) Key role of coupling, delay, and noise in resting brain fluctuations. *Proc Natl Acad Sci USA* 106:10302–10307
- Deco GR, Jirsa VK, McIntosh AR (2011) Emerging concepts for the dynamical organization of resting-state activity in the brain. *Nat Rev Neurosci* 12:43–56
- Deneux T, Faugeras O (2010) EEG-fMRI fusion of paradigm-free activity using Kalman filtering. *Neural Comput* 22:906–948
- Dienel GA, Cruz NF (2003) Neighborly interactions of metabolically-activated astrocytes in vivo. *Neurochem Int* 43:339–354
- Dutta S, Matsumoto Y, Gothgen NU, Ebling WF (1997) Concentration-EEG effect relationship of propofol in rats. *J Pharm Sci* 86:37–43
- Eccles JC (1992) Evolution of consciousness. *Proc Natl Acad Sci USA* 89:7320–7324
- Ermentrout BG (1998) Neural networks as spatio-temporal pattern-forming systems. *Rep Prog Phys* 61:353–430
- Faugeras O, Touboul J, Cessac B (2009) A constructive mean-field analysis of multi-population neural networks with random synaptic weights and stochastic inputs. *Front Comput Neurosci* 3:1
- Feshchenko VA, Veselis RA, Reinsel RA (2004) Propofol-induced alpha rhythm. *Neuropsychobiology* 50:257–266
- Fleischhauer K, Petsche H, Wittkowski W (1972) Vertical bundles of dendrites in the neocortex. *Z Anat Entwicklungsgesch* 136:213–223
- Foster BL, Bojak I, Liley DTJ (2008) Population based models of cortical drug response: insights from anaesthesia. *Cogn Neurodyn* 2:283–296
- Frascoli F, van Veen L, Bojak I, Liley DTJ (2011) Metabifurcation analysis of a mean field model of the cortex. *Physica D* 240:949–962. doi:10.1016/j.physd.2011.02.002
- Freeman WJ (1975) Mass action in the nervous system: examination of the neurophysiological basis of adaptive behavior through the EEG, 1st edn. Academic Press, New York, also electronic edn.: <http://sulcus.berkeley.edu/MANSWWW/MANSWWW.html>, 2004
- Freeman WJ (1979) Nonlinear gain mediating cortical stimulus-response relations. *Biol Cybern* 33:237–247
- Freeman WJ, Holmes MD (2005) Metastability, instability, and state transition in neocortex. *Neural Netw* 18:497–504
- Freeman WJ, Ahlfors SP, Menon V (2009) Combining fMRI with EEG and MEG in order to relate patterns of brain activity to cognition. *Int J Psychophysiol* 73:43–52
- Friston KJ (1997) Transients, metastability, and neuronal dynamics. *NeuroImage* 5:164–171
- Friston KJ (2000) The labile brain. I. Neuronal transients and nonlinear coupling. *Philos Trans R Soc B* 355:215–236
- Friston KJ (2002) Bayesian estimation of dynamical systems: an application to fMRI. *NeuroImage* 16:513–530
- Friston KJ, Mechelli A, Turner R, Price CJ (2000) Nonlinear responses in fMRI: The Balloon model, Volterra kernels, and other hemodynamics. *NeuroImage* 12:466–477
- Friston KJ, Penny WD, Phillips C, Kiebel SJ, Hinton GE, Ashburner J (2002) Classical and Bayesian inference in neuroimaging: theory. *NeuroImage* 16:465–483
- Friston KJ, Harrison LM, Penny WD (2003) Dynamic causal modelling. *NeuroImage* 19:1273–1302
- Friston KJ, Mattout J, Trujillo-Barreto NJ, Ashburner J, Penny WD (2007) Variational free energy and the Laplace approximation. *NeuroImage* 34:220–234
- Ghosh A, Rho YA, McIntosh AR, Kötter R, Jirsa VK (2008) Noise during rest enables the exploration of the brain's dynamic repertoire. *PLoS Comput Biol* 4:e1000196
- Gloor P (1969) Hans Berger on the electroencephalogram of man. *Electroencephalogr Clin Neurophysiol* S28:350

- Goldman PS, Nauta WJH (1977) Columnar distribution of cortico-cortical fibers in the frontal association, limbic, and motor cortex of the developing rhesus monkey. *Brain Res* 122: 393–413
- Griffith JS (1963) A field theory of neural nets: I: derivation of field equations. *Bull Math Biol* 25:111–120
- Griffith JS (1965) A field theory of neural nets: II: properties of the field equations. *Bull Math Biol* 27:187–195
- Hagmann P, Cammoun L, Gigandet X, Meuli RA, Wedeen VJ, Sporns O (2008) Mapping the structural core of human cerebral cortex. *PLoS Biol* 6:e159
- Haken H (1983) *Synergetics: an introduction. Nonequilibrium phase transitions and self-organization in physics, chemistry, and biology*, 3rd edn. Springer, Berlin
- Hellwig B (2000) A quantitative analysis of the local connectivity between pyramidal neurons in layers 2/3 of the rat visual cortex. *Biol Cybern* 82:111–121
- Herculano-Houzel S (2009) The human brain in numbers: a linearly scaled-up primate brain. *Front Hum Neurosci* 3:31
- Honey CJ, Kötter R, Breakspear M, Sporns O (2007) Network structure of cerebral cortex shapes functional connectivity on multiple time scales. *Proc Natl Acad Sci USA* 104:10240–10245
- Honey CJ, Sporns O, Cammoun L, Gigandet X, Thiran JP, Meuli RA, Hagmann P (2009) Predicting human resting-state functional connectivity from structural connectivity. *Proc Natl Acad Sci USA* 106:2035–2040
- Hughes SW, Crunelli V (2005) Thalamic mechanisms of EEG alpha rhythms and their pathological implications. *Neuroscientist* 11:357–372
- Hughes SW, Crunelli V (2007) Just a phase they're going through: the complex interaction of intrinsic high-threshold bursting and gap junctions in the generation of thalamic alpha and theta rhythms. *Int J Psychophysiol* 64:3–17
- Hutt A, Longtin A (2010) Effects of the anesthetic agent propofol on neural populations. *Cogn Neurodyn* 4:37–59
- Jansen BH, Rit VG (1995) Electroencephalogram and visual evoked potential generation in a mathematical model of coupled cortical columns. *Biol Cybern* 73:357–366
- Jirsa VK, Haken H (1996) Field theory of electromagnetic brain activity. *Phys Rev Lett* 77: 960–963
- Jirsa VK, Jantzen KJ, Fuchs A, Kelso JAS (2002) Spatiotemporal forward solution of the EEG and MEG using network modeling. *IEEE Trans Med Imaging* 21:493–504
- Johansen-Berg H, Rushworth MFS (2009) Using diffusion imaging to study human connective anatomy. *Annu Rev Neurosci* 32:75–94
- Jones EG (2000) Microcolumns in the cerebral cortex. *Proc Natl Acad Sci USA* 97:5019–5021
- Jones EG, Burton H, Porter R (1975) Commissural and cortico-cortical “columns” in the somatic sensory cortex of primates. *Science* 190:572–574
- Kaiser M, Hilgetag CC, van Ooyen A (2009) A simple rule for axon outgrowth and synaptic competition generates realistic connection lengths and filling fractions. *Cereb Cortex* 19: 3001–3010
- Kandel ER, Schwartz JH, Jessell TM (2000) *Principles of neural science*, 4th edn. McGraw-Hill, New York
- Kelso JAS (1995) *Dynamic patterns: the self-organization of brain and behavior*. The MIT Press, Cambridge
- Kiebel SJ, David O, Friston KJ (2006) Dynamic causal modelling of evoked responses in EEG/MEG with lead field parameterization. *NeuroImage* 30:1273–1284
- Kim JS, Singh V, Lee JK, Lerch J, Ad-Dab'bagh Y, MacDonald DJ, Lee JM, Kim SI, Evans AC (2005) Automated 3-D extraction and evaluation of the inner and outer cortical surfaces using a Laplacian map and partial volume effect classification. *NeuroImage* 27:210–221
- Kötter R, Wanke E (2005) Mapping brains without coordinates. *Philos Trans R Soc B* 360:751–766
- Kramer MA, Kirsch HE, Szeri AJ (2005) Pathological pattern formation and cortical propagation of epileptic seizures. *J R Soc Interface* 2:113–127

- Kuizenga K, Kalkman CJ, Hennis PJ (1998) Quantitative electroencephalographic analysis of the biphasic concentration-effect relationship of propofol in surgical patients during extradural analgesia. *Br J Anaesth* 80:725–732
- Kuizenga K, Wierda JMKH, Kalkman CJ (2001) Biphasic EEG changes in relation to loss of consciousness during induction with thiopental, propofol, etomidate, midazolam or sevoflurane. *Br J Anaesth* 86:354–360
- Laufs H, Daunizeau J, Carmichael DW, Kleinschmidt AK (2008) Recent advances in recording electrophysiological data simultaneously with magnetic resonance imaging. *NeuroImage* 40:515–528
- Liley DTJ, Bojak I (2005) Understanding the transition to seizure by modeling the epileptiform activity of general anesthetic agents. *J Clin Neurophysiol* 22:300–313
- Liley DTJ, Wright JJ (1994) Intracortical connectivity of pyramidal and stellate cells: estimates of synaptic densities and coupling symmetry. *Netw Comput Neural Syst* 5:175–189
- Liley DTJ, Alexander DM, Wright JJ, Aldous MD (1999a) Alpha rhythm emerges from large-scale networks of realistically coupled multicompartmental model cortical neurons. *Netw Comput Neural Syst* 10:79–92
- Liley DTJ, Cadusch PJ, Wright JJ (1999b) A continuum theory of electro-cortical activity. *Neurocomputing* 26-27:795–800
- Liley DTJ, Cadusch PJ, Dafilis MP (2002) A spatially continuous mean field theory of electrocortical activity. *Netw Comput Neural Syst* 13:67–113
- Liley DTJ, Cadusch PJ, Dafilis MP (2003) Corrigendum. *Netw Comput Neural Syst* 14:369
- Liley DTJ, Cadusch PJ, Gray M, Nathan PJ (2003b) Drug-induced modification of the system properties associated with spontaneous human electroencephalographic activity. *Phys Rev E* 68:05190
- Liley DTJ, Bojak I, Dafilis MP, van Veen L, Frascoli F, Foster BL (2010) Bifurcations and state changes in the human alpha rhythm: theory and experiment. In: Steyn-Ross DA, Steyn-Ross ML (eds) *Modeling phase transitions in the brain*. Springer series in computational neuroscience, vol 4. Springer, New York, pp 117–145
- Liley DTJ, Foster BL, Bojak I (2011) A mesoscopic modelling approach to anaesthetic action on brain electrical activity. In: Hutt A (ed) *Sleep and anesthesia: neural correlates in theory and experiment*. Springer series in computational neuroscience, vol 15. Springer, New York, pp 139–166
- Linás RR (1988) The intrinsic electrophysiological properties of mammalian neurons: insights into central nervous system function. *Science* 242:1654–1664
- Logothetis NK (2008) What we can do and what we cannot do with fMRI. *Nature* 453:869–878
- Lopes da Silva FH, Hoeks A, Smits H, Zetterberg LH (1974) Model of brain rhythmic activity: the alpha-rhythm of the thalamus. *Kybernetik* 15:27–37
- Lopes da Silva FH, Blanes W, Kalitzin SN, Parra J, Suffczyński P, Velis DN (2003) Dynamical diseases of brain systems: different routes to epileptic seizures. *IEEE Trans Biomed Eng* 50:540–548
- López-Muñoz F, Boya J, Alamo C (2006) Neuron theory, the cornerstone of neuroscience, on the centenary of the Nobel Prize award to Santiago Ramón y Cajal. *Brain Res Bull* 70:391–405
- Lübke J, Feldmeyer D (2007) Excitatory signal flow and connectivity in a cortical column: focus on barrel cortex. *Brain Struct Funct* 212:3–17
- Mandeville JB, Marota JJA, Ayata C, Zaharchuk G, Moskowitz MA, Rosen BR, Weisskoff RM (1999) Evidence of a cerebrovascular postarteriole windkessel with delayed compliance. *J Cereb Blood Flow Metab* 19:679–689
- Marder E, Taylor AL (2011) Multiple models to capture the variability in biological neurons and networks. *Nat Neurosci* 14:133–138
- Markram H (2006) The blue brain project. *Nat Rev Neurosci* 7:153–160
- Markram H (2008) Fixing the location and dimensions of functional neocortical columns. *HFSP J* 2:132–135
- Markram H, Toledo-Rodriguez M, Wang Y, Gupta A, Silberberg G, Wu C (2004) Interneurons of the neocortical inhibitory system. *Nat Rev Neurosci* 5:793–807

- Marten F, Rodrigues S, Benjamin O, Richardson MP, Terry JR (2009) Onset of polyspike complexes in a mean-field model of human electroencephalography and its application to absence epilepsy. *Philos Trans R Soc A* 367:1145–1161
- Matthews PM, Honey GD, Bullmore ET (2006) Applications of fMRI in translational medicine and clinical practice. *Nat Rev Neurosci* 7:732–744
- Mavritsaki E, Heinke D, Allen H, Deco GR, Humphreys GW (2011) Bridging the gap between physiology and behavior: Evidence from the sSoTS model of human visual attention. *Psychol Rev* 118:3–41
- McCulloch WS, Pitts W (1943) A logical calculus of the ideas immanent in nervous activity. *Bull Math Biophys* 5:115–133, reprinted 1990 in *Bull Math Biol* 52: 99–115
- Miguel-Hidalgo JJ (2005) Lower packing density of glial fibrillary acidic protein-immunoreactive astrocytes in the prelimbic cortex of alcohol-naive and alcohol-drinking alcohol-preferring rats as compared with alcohol-nonpreferring and Wistar rats. *Alcohol Clin Exp Res* 29:766–772
- Molae-Ardekani B, Senhadji L, Shamsollahi MB, Vosoughi-Vahdat B, Wodey E (2007) Brain activity modeling in general anesthesia: enhancing local mean-field models using a slow adaptive firing rate. *Phys Rev E* 76:041911
- Molae-Ardekani B, Benquet P, Bartolomei F, Wendling F (2010) Computational modeling of high-frequency oscillations at the onset of neocortical partial seizures: from ‘altered structure’ to ‘dysfunction’. *NeuroImage* 52:1109–1122
- Moran RJ, Kiebel SJ, Stephan KE, Reilly RB, Daunizeau J, Friston KJ (2007) A neural mass model of spectral responses in electrophysiology. *NeuroImage* 37:706–720
- Moran RJ, Stephan KE, Kiebel SJ, Rombach N, OConnor WT, Murphy KJ, Reilly RB, Friston KJ (2008) Bayesian estimation of synaptic physiology from the spectral responses of neural masses. *NeuroImage* 42:272–284
- Moran RJ, Stephan KE, Seidenbecher T, Pape HC, Dolan RJ, Friston KJ (2009) Dynamic causal models of steady-state responses. *NeuroImage* 44:796–811
- Mori S, Wakana S, van Zijl PCM, Nagae-Poetscher LM (2005) MRI atlas of human white matter. Elsevier, Amsterdam
- Mountcastle VB (1957) Modality and topographic properties of single neurons of cat’s somatic sensory cortex. *J Neurophysiol* 20:408–434
- Mountcastle VB (1979) An organizing principle for cerebral function: the unit module and the distributed system. In: Schmitt FO, Worden FG (eds) *The neurosciences: fourth study program*. The MIT Press, Cambridge, pp 21–42
- Mountcastle VB (1997) The columnar organization of the neocortex. *Brain* 120:701–722
- Mulert C, Pogarell O, Hegerl U (2008) Simultaneous EEG-fMRI: perspectives in psychiatry. *Clin EEG Neurosci* 39:61–64
- Musso F, Brinkmeyer J, Mobascher A, Warbrick T, Winterer G (2010) Spontaneous brain activity and EEG microstates. A novel EEG/fMRI analysis approach to explore resting-state networks. *NeuroImage* 52:1149–1161
- Niedermeyer E, Lopes da Silva FH (eds) (2005) *Electroencephalography: Basic principles, clinical applications, and related fields*, 5th edn. Lippincott Williams & Wilkins, Philadelphia
- Nieuwenhuys R, Voogd J, van Huijzen C (2008) *The human central nervous system*, 4th edn. Springer, Berlin, pp 491–679
- Norris DG (2006) Principles of magnetic resonance assessment of brain function. *J Magn Reson Imaging* 23:794–807
- Nunez PL (1974a) The brain wave equation: a model for the EEG. *Math Biosci* 21:279–297
- Nunez PL (1974b) Wave-like properties of the alpha rhythm. *IEEE Trans Biomed Eng* 21:473–482
- Nunez PL (1981) *Electric fields of the brain: the neurophysics of EEG*, 1st edn. Oxford University Press, New York
- Nunez PL (1995) *Neocortical dynamics and human EEG rhythms*. Oxford University Press, New York
- Nunez PL, Srinivasan R (2006) A theoretical basis for standing and traveling brain waves measured with human EEG with implications for an integrated consciousness. *Clin Neurophysiol* 117:2424–2435

- Nunez PL, Reid L, Bickford RG (1978) The relationship of head size to alpha frequency with implications to a brain wave model. *Electroencephalogr Clin Neurophysiol* 44:344–352
- Nunez PL, Wingeier BM, Silberstein RB (2001) Spatial-temporal structures of human alpha rhythms: theory, microcurrent sources, multiscale measurements, and global binding of local networks. *Hum Brain Mapp* 13:125–164
- Pakkenberg B, Gundersen HJG (1997) Neocortical neuron number in humans: effect of sex and age. *J Comp Neurol* 384:312–320
- Perea G, Araque A (2010) GLIA modulates synaptic transmission. *Brain Res Rev* 63:93–102
- Perea G, Navarrete M, Araque A (2009) Tripartite synapses: astrocytes process and control synaptic information. *Trends Neurosci* 32:421–431
- Peters A, Sethares C (1997) The organization of double bouquet cells in monkey striate cortex. *J Neurocytol* 26:779–797
- Petersen CCH (2007) The functional organization of the barrel cortex. *Neuron* 56:339–355
- Phillips AJK, Robinson PA (2007) A quantitative model of sleep-wake dynamics based on the physiology of the brainstem ascending arousal system. *J Biol Rhythms* 22:167–179
- Rabinovich MI, Huerta R, Laurent G (2008a) Neuroscience. Transient dynamics for neural processing. *Science* 321:48–50
- Rabinovich MI, Huerta R, Varona P, Afraimovich VS (2008b) Transient cognitive dynamics, metastability, and decision making. *PLoS Comput Biol* 4:e1000072
- Raichle ME, MacLeod AM, Snyder AZ, Powers WJ, Gusnard DA, Shulman GL (2001) A default mode of brain function. *Proc Natl Acad Sci USA* 98:676–682
- Regan D (1989) Human brain electrophysiology: evoked potentials and evoked magnetic fields in science and medicine. Elsevier, New York
- Rennie CJ, Wright JJ, Robinson PA (2000) Mechanisms of cortical electrical activity and emergence of gamma rhythm. *J Theor Biol* 205:17–35
- Rennie CJ, Robinson PA, Wright JJ (2002) Unified neurophysical model of EEG spectra and evoked potentials. *Biol Cybern* 86:457–471
- Riera JJ, Aubert E, Iwata K, Kawashima R, Wan X, Ozaki T (2005) Fusing EEG and fMRI based on a bottom-up model: inferring activation and effective connectivity in neural masses. *Philos Trans R Soc B* 360:1025–1041
- Riera JJ, Wan X, Jimenez JC, Kawashima R (2006) Nonlinear local electrovascular coupling. I: a theoretical model. *Hum Brain Mapp* 27:896–914
- Riera JJ, Jimenez JC, Wan X, Kawashima R, Ozaki T (2007) Nonlinear local electrovascular coupling. II: from data to neuronal masses. *Hum Brain Mapp* 28:335–354
- Robinson PA (2006) Patchy propagators, brain dynamics, and the generation of spatially structured gamma oscillations. *Phys Rev E* 73:041904
- Robinson PA, Rennie CJ, Wright JJ (1997) Propagation and stability of waves of electrical activity in the cerebral cortex. *Phys Rev E* 56:826–840
- Robinson PA, Rennie CJ, Wright JJ, Bahramali H, Gordon E, Rowe DL (2001) Prediction of electroencephalographic spectra from neurophysiology. *Phys Rev E* 63:021903
- Robinson PA, Rennie CJ, Rowe DL (2002) Dynamics of large-scale brain activity in normal arousal states and epileptic seizures. *Phys Rev E* 65:041924
- Rockland KS, Ichinohe N (2004) Some thoughts on cortical minicolumns. *Exp Brain Res* 158:265–277
- Rockland KS, Pandya DN (1979) Laminar origins and terminations of cortical connections of the occipital lobe in the rhesus monkey. *Brain Res* 179:3–20
- Rodrigues S, Terry JR, Breakspear M (2006) On the genesis of spike-wave oscillations in a mean-field model of human thalamic and corticothalamic dynamics. *Phys Lett A* 355:352–357
- Rowe DL, Robinson PA, Gordon E (2005) Stimulant drug action in attention deficit hyperactivity disorder (ADHD): inference of neurophysiological mechanisms via quantitative modelling. *Clin Neurophysiol* 116:324–335
- Scheperjans F, Eickhoff SB, Hömke L, Mohlberg H, Hermann K, Amunts K, Zilles K (2008) Probabilistic maps, morphometry, and variability of cytoarchitectonic areas in the human superior parietal cortex. *Cereb Cortex* 18:2141–2157

- Shibasaki H (2008) Human brain mapping: hemodynamic response and electrophysiology. *Clin Neurophysiol* 119:731–743
- Silva LR, Amitai Y, Connors BW (1991) Intrinsic oscillations of neocortex generated by layer 5 pyramidal neurons. *Science* 251:432–435
- Sotero RC, Trujillo-Barreto NJ (2008) Biophysical model for integrating neuronal activity, EEG, fMRI and metabolism. *NeuroImage* 39:290–309
- Sotero RC, Trujillo-Barreto NJ, Iturria-Medina Y, Carbonell F, Jimenez JC (2007) Realistically coupled neural mass models can generate EEG rhythms. *Neural Comput* 19:478–512
- Spiegler A, Kiebel SJ, Atay FM, Knösche TR (2010) Bifurcation analysis of neural mass models: impact of extrinsic inputs and dendritic time constants. *NeuroImage* 52:1041–1058
- Spruston N (2008) Pyramidal neurons: dendritic structure and synaptic integration. *Nat Rev Neurosci* 9:206–221
- Stam CJ (2005) Nonlinear dynamical analysis of EEG and MEG: review of an emerging field. *Clin Neurophysiol* 116:2266–2301
- Stam CJ, Pijn JPM, Suffczyński P, Lopes da Silva FH (1999) Dynamics of the human alpha rhythm: evidence for non-linearity? *Clin Neurophysiol* 110:1801–1813
- Stephan KE, Kamper L, Bozkurt A, Burns GAPC, Young MP, Kötter R (2001) Advanced database methodology for the collation of connectivity data on the macaque brain (CoCoMac). *Philos Trans R Soc B* 356:1159–1186
- Steriade M (2005) Cellular substrates of brain rhythms. In: Niedermeyer E, Lopes da Silva FH (eds) *Electroencephalography: basic principles, clinical applications, and related fields*, 5th edn. Lippincott Williams & Wilkins, Philadelphia, pp 31–83
- Steyn-Ross ML, Steyn-Ross DA, Sleight JW, Liley DTJ (1999) Theoretical electroencephalogram stationary spectrum for a white-noise-driven cortex: evidence for a general anesthetic-induced phase transition. *Phys Rev E* 60:7299–7311
- Steyn-Ross ML, Steyn-Ross DA, Sleight JW (2004) Modelling general anaesthesia as a first-order phase transition in the cortex. *Prog Biophys Mol Biol* 85:369–385
- Steyn-Ross DA, Steyn-Ross ML, Sleight JW, Wilson MT, Gillies IP, Wright JJ (2005a) The sleep cycle modelled as a cortical phase transition. *J Biol Phys* 31:547–569
- Steyn-Ross ML, Steyn-Ross DA, Sleight JW, Wilson MT, Wilcocks LC (2005b) Proposed mechanism for learning and memory erasure in a white-noise-driven sleeping cortex. *Phys Rev E* 72:061910
- Steyn-Ross ML, Steyn-Ross DA, Wilson MT, Sleight JW (2009) Modeling brain activation patterns for the default and cognitive states. *NeuroImage* 45:298–311
- Steyn-Ross ML, Steyn-Ross DA, Sleight JW, Wilson MT (2011) A mechanism for ultra-slow oscillations in the cortical default network. *Bull Math Biol* (in press). doi:10.1007/s11538-010-9565-9
- Stufflebeam SM, Rosen BR (2007) Mapping cognitive function. *Neuroimaging Clin N Am* 17:469–484
- Suffczyński P, Lopes da Silva FH, Parra J, Velis DN, Kalitzin SN (2005) Epileptic transitions: model predictions and experimental validation. *J Clin Neurophysiol* 22:288–299
- Szentágothai J (1978) The Ferrier lecture, 1977 – the neuron network of the cerebral cortex: a functional interpretation. *Proc R Soc Lond B* 201:219–248
- Szentágothai J (1983) The modular architectonic principle of neural centers. *Rev Physiol Biochem Pharmacol* 98:11–61
- Tang Y, Nyengaard JR, De Groot DM, Gundersen HJG (2001) Total regional and global number of synapses in the human brain neocortex. *Synapse* 41:258–273
- Thomson AM, Bannister AP (2003) Interlaminar connections in the neocortex. *Cereb Cortex* 13:5–14
- Toga AW, Thompson PM, Mori S, Amunts K, Zilles K (2006) Towards multimodal atlases of the human brain. *Nat Rev Neurosci* 7:952–966
- Tsuda I (2001) Toward an interpretation of dynamic neural activity in terms of chaotic dynamical systems. *Behav Brain Sci* 24:793–810

- Valdés-Hernández PA, Ojeda-González A, Martínez-Montes E, Lage-Castellanos A, Virués-Alba T, Valdés-Urrutia L, Valdes-Sosa PA (2010) White matter architecture rather than cortical surface area correlates with the EEG alpha rhythm. *NeuroImage* 49:2328–2339
- Valdes-Sosa PA, Sánchez-Bornot JM, Sotero RC, Iturria-Medina Y, Alemán-Gómez Y, Bosch-Bayard J, Carbonell F, Ozaki T (2009) Model driven EEG/fMRI fusion of brain oscillations. *Hum Brain Mapp* 30:2701–2721
- van Albada SJ, Robinson PA (2009) Mean-field modeling of the basal ganglia-thalamocortical system. I. Firing rates in healthy and Parkinsonian states. *J Theor Biol* 257:642–663
- Van Essen DC (2005) A Population-Average, Landmark- and Surface-based (PALS) atlas of human cerebral cortex. *NeuroImage* 28:635–662
- van Rotterdam A, Lopes da Silva FH, van den Ende J, Viergever MA, Hermans AJ (1982) A model of the spatial-temporal characteristics of the alpha rhythm. *Bull Math Biol* 44:283–305
- Waage P, Guldberg CM, Abrash HI (1986) Studies concerning affinity (English translation). *J Chem Educ* 63:1044–1047
- Wendling F, Bellanger JJ, Bartolomei F, Chauvel PY (2000) Relevance of nonlinear lumped-parameter models in the analysis of depth-EEG epileptic signals. *Biol Cybern* 83:367–378
- Wendling F, Hernández AI, Bellanger JJ, Chauvel PY, Bartolomei F (2005) Interictal to ictal transition in human temporal lobe epilepsy: insights from a computational model of intracerebral EEG. *J Clin Neurophysiol* 22:343–356
- White EL (1989) Cortical circuits. Synaptic organization of the cerebral cortex: structure, function and theory. Birkhäuser, Boston
- Williamson SJ, Kaufman L (1989) Advances in neuromagnetic instrumentation and studies of spontaneous brain activity. *Brain Topogr* 2:129–139
- Wilson HR, Cowan JD (1972) Excitatory and inhibitory interactions in localized populations of model neuron. *Biophys J* 12:1–24
- Wilson HR, Cowan JD (1973) A mathematical theory of the functional dynamics of cortical and thalamic nervous tissue. *Kybernetik* 13:55–80
- Wilson MT, Steyn-Ross DA, Sleight JW, Steyn-Ross ML, Wilcocks LC, Gillies IP (2006) The K-complex and slow oscillation in terms of a mean-field cortical model. *J Comput Neurosci* 21:243–257
- Wilson MT, Steyn-Ross ML, Steyn-Ross DA, Sleight JW (2007) Going beyond a mean-field model for the learning cortex: second-order statistics. *J Biol Phys* 33:213–246
- Wolfe J, Houweling AR, Brecht M (2010) Sparse and powerful cortical spikes. *Curr Opin Neurobiol* 20:306–312
- Wright JJ (1997) EEG simulation: variation of spectral envelope, pulse synchrony and ≈ 40 hz oscillation. *Biol Cybern* 76:181–194
- Wright JJ, Liley DTJ (1995) Simulation of electrocortical waves. *Biol Cybern* 72:347–356
- Wright JJ, Liley DTJ (1996) Dynamics of the brain at global and microscopic scales: neural networks and the EEG. *Behav Brain Sci* 19:285–320
- Wu JY, Huang XY, Zhang C (2008) Propagating waves of activity in the neocortex: what they are, what they do. *Neuroscientist* 14:487–502
- Zilles K, Amunts K (2010) Centenary of Brodmann's map – conception and fate. *Nat Rev Neurosci* 11:139–145